# Studies on the *Escherichia coli* ExbD Transmembrane Domain, Residue L132, and an Inhibitory Cyclic Peptide.

Bimal Jana[1,3], Dale Kopp[1,4], Mingchao Xie[1,5], Hema Vakharia-Rao[2,6] and Kathleen Postle[1,2]*

RUNNING TITLE:

ExbD homodimerizes through its transmembrane domain.

KEYWORDS:

ExbD, TonB, energy transduction, disulfide bond, membrane protein, protonmotive force, *Escherichia coli*

[1]Department of Biochemistry and Molecular Biology, The Pennsylvania State University, University Park, PA, 16802, USA

[2]School of Molecular Biosciences, Washington State University, Pullman, WA 99164

*Address correspondence to Kathleen Postle at postle@psu.edu

Current addresses:

[3]Center for Genomic Medicine, Massachusetts General Hospital, Boston, MA 02114, USA

[4] Bristol Myers Squib, Bothell, WA 98021

[5]AstraZeneca, Waltham, MA, USA

[6] Bangalore 560016 India

## ABSTRACT

The TonB system of *Escherichia coli* uses the cytoplasmic membrane protonmotive force (PMF) to energize active transport of nutrients across the otherwise unenergized outer membrane. Because it overcomes limitations for nutrient diffusion through outer membrane size-limiting porins, it provides a growth advantage and is widespread among Gram-negative bacteria. It consists of three known cytoplasmic membrane proteins, TonB, ExbB and ExbD that energize a variety of customized TonB-dependent transporters in the outer membrane. The sole ExbD transmembrane domain is proposed to consist of residues 23-43 (Kampfenkel and Braun, 1992, J. Bacteriol. 174:5485-7). Here we showed that the charge and location of residue Asp25 were essential for activity of the TonB system, thus identifying it as the only PMF-responsive element in the TonB system. The proposed boundaries of the transmembrane domain α-helix were revised to consist of residues 23-39, with residues 40-43 initiating the subsequent disordered region required for signal transduction (Kopp and Postle, 2020, J. Bacteriol. 202, e00687-19). Trapping of disulfide-linked ExbD homodimers through T42C or V43C prevented TonB system activity that was restored by addition of the reducing agent dithiothreitol, indicating a requirement for motion. In *vivo* photo-cross-linking experiments suggested that motion was rotation of ExbD transmembrane domains. Inactivity of ExbD L132Q, the first ExbD mutant identified, was likely due to steric hindrance. A conserved and defined site of *in vivo* ExbD interaction with TonB was identified. Exogenous addition of a cyclic peptide based on that site inhibited ExbD-TonB interaction while concomitantly decreasing iron transport efficiency. This suggested that a novel antimicrobial strategy against ESKAPE and other Gram-negative pathogens could be developed by targeting ExbD protein-protein interactions.

57 **INTRODUCTION**

58 Gram-negative bacteria are characterized by their distinctive outer membranes that serve as
59 intrinsic barriers to environmental agents, antibiotics, and degradative enzymes. To overcome the
60 concomitant nutrient limitations imposed by the outer membrane, the TonB system energizes transport
61 across the outer membrane of a wide array of scarce, important nutrients such as iron-siderophores,
62 heme, zinc, copper, cobalamin, nickel, maltodextrin, chitin oligosaccharides, and sucrose [for reviews
63 see (1-8)]. The TonB system is also an essential component for pathogenesis by certain Gram-negative
64 bacteria (9).

65 In *Escherichia coli* K12 the TonB-dependent transport ligands are iron-siderophores and
66 cobalamin. The TonB system consists of integral cytoplasmic membrane proteins ExbB and ExbD,
67 which harvest the protonmotive force (PMF) of the cytoplasmic membrane, and transmit it to the
68 integral cytoplasmic membrane protein TonB, which then transmits mechanical energy to customized β-
69 barrels in the outer membrane known as TonB-dependent transporters (TBDTs) (Fig.1). In the absence
70 of PMF or TonB, ligands bind to TBDTs but do not cross the outer membrane or enter the periplasm.
71 Because the TBDTs greatly outnumber TonB and compete for contact with it, it is likely that TonB
72 engages in an energy transduction cycle involving transient interactions with individual TBDTs (10-12).

73 Structurally, the TBDT β-barrels consist of 22 strands, with a lumen that is occluded by an
74 amino-terminal globular domain, called the cork or hatch. *In vivo*, the periplasmically exposed surface
75 of the TBDT appears to signal that ligand is bound via a conformational change that allows for
76 productive interaction with TonB (13-18). The cork domain moves *in vivo* during contact with TonB
77 (18).

78 Among the three integral cytoplasmic membrane proteins in the TonB system, there are five
79 transmembrane domains, any one of which could theoretically respond to the PMF of the cytoplasmic
80 membrane. TonB and ExbD are both anchored by a single transmembrane domain with the majority of
81 each protein occupying the periplasmic space (Fig.1) [(19-21). ExbB has three transmembrane domains,

82 with an N-out, C-in topology and primarily occupies the cytoplasm (22). TonB and ExbD both depend
83 on ExbB for their proteolytic stability suggesting that ExbB constitutes a scaffolding for their assembly
84 [(23-25); unpublished results]. Consistent with that idea, the cellular ratio of TonB:ExbD:ExbB is 1:2:7
85 (11). The TonB transmembrane domain remains homodimerized throughout the energy transduction
86 cycle, thus making the ratio 2:4:14 (12). Our current model suggests that, as TonB initiates an energy
87 transduction cycle, its previously monomeric periplasmic domain becomes a homodimer, that can then
88 interact with ExbD homodimerized through its periplasmic domain; this transforms into a TonB-ExbD
89 heterodimer that subsequently configures TonB to energize active transport of nutrients through a TBDT
90 (Fig. 2). In this model the proposed energy-dependent step is recycling of ExbD homodimers to an
91 energized state.

92 The sole potentially PMF-responsive residue in the TonB transmembrane domain, His20, can be
93 fully functionally replaced by a non-protonatable Asparagine residue, thus removing it from
94 consideration as part of the mechanism of energy transduction (26). Likewise, all of the potentially
95 PMF-responsive residues in the three ExbB transmembrane domains are excluded because non-
96 protonatable substitutions are active (27). This leaves Asp25 in the ExbD transmembrane domain as the
97 sole actor that could potentially mediate PMF-dependence in the TonB system.

98 Because both active and inactive TonBs can bind to TBDTs that are both ligand-bound and
99 ligand-free both *in vivo* and *in vitro*, energy transduction cannot be explained by simple binding (14, 28-
100 34). Only *in vivo* full-length active TonB leads to active transport of ligands through a TBDT,
101 suggesting that there must be a difference in the residues through which the active and inactive TonBs
102 bind TBDTs. That difference appears to be manifested by the ability of TonB to interact correctly with
103 PMF-activated ExbD such that it achieves an "energized" conformation.

104 10-residue deletion scanning suggests that all ExbD residues are functionally important except
105 for a few amino acids at the cytoplasmic amino terminus (35). ExbD makes multiple *in vivo* contacts
106 during TonB-dependent energy transduction, including formaldehyde cross-linked ExbD-ExbD

107 homodimers, and ExbD-ExbB and ExbD-TonB heterodimers. Consistent with the formaldehyde cross-
108 linking studies, the ExbD periplasmic domain forms a disulfide cross-linked ExbD-ExbD homodimer
109 and ExbD-TonB heterodimer *in vivo*, with nearly the same ExbD residues involved in both complexes
110 (36). In contrast, TonB is essentially impervious to missense mutations, with H20 in the transmembrane
111 domain playing only a structural role [(26, 37-41); Potter and Postle, unpublished results]. Thus, TonB
112 appears to be a puppet with ExbD as the puppet-master.

113 The role of ExbD can be recapitulated in spheroplasts, which retain their PMF, as well as all of
114 the elements of the cytoplasm that the TonB system may require. The conformation of ExbD is PMF-
115 dependent and it is only by interaction with ExbD that TonB conformations respond to PMF (42).

116 There have been several indications as to the importance of ExbD Asp 25. ExbD D25N
117 inactivates ExbD (and thus the entire TonB system) and is dominant negative, consistent with being part
118 of a multiprotein complex (43). ExbD D25N mimics the effect of PMF collapse that prevents the ExbD-
119 TonB interaction characterized by *in vivo* formaldehyde cross-linking (29). In the proposed TonB
120 energy transduction cycle, ExbD D25N stalls the ExbD-TonB periplasmic domain interaction at Stage
121 II, the energy-independent stage, such that it cannot proceed to the energy-dependent ExbD-TonB
122 interaction [Fig. 2; (29, 36, 42-44)]. Like wild-type ExbD, ExbD D25N formaldehyde-cross-links
123 normally with ExbB monomer and forms homodimers *in vivo* (29).

124 Along with ExbD, MotB and TolQ participate in three paralogous cytoplasmic membrane
125 systems in *E. coli* K12. Each of the systems uses PMF to energize events at the outer membrane and has
126 two cytoplasmic membrane components in common: one protein with multiple transmembrane domains,
127 occupying primarily the cytoplasm (ExbB, TolQ, and MotA), and one protein anchored by a single
128 transmembrane domain, occupying primarily the periplasm (ExbD, TolR, and MotB) (45-48). TolR and
129 MotB carry an essential Asp residue in their single transmembrane domain at positions 23 and 32
130 respectively (47, 49), suggesting that ExbD Asp 25 might be equally important.

131 Here we present a detailed analysis of the ExbD transmembrane domain indicating the pivotal
132 role both charge and location of Asp25 play in TonB system response to cytoplasmic membrane PMF.
133 We redefine the boundaries of the transmembrane domain and identify an subsequent adjacent segment
134 that initiates a previously characterized disordered domain. We show that the ExbD transmembrane
135 domains homodimerize, appear to rotate relative to one another, and that, if dynamic movement is
136 prevented by disulfide trapping, ExbD ceases to function. These results suggest that the snapshots of
137 ExbB/D and MotA/B provided by recent cryo-EM structures do not yet capture the mechanism by which
138 they utilize the PMF (50-52). We also exclude the overall importance of ExbD L132, first identified as
139 an inactive L132Q missense mutation, showing that several different amino acids can functionally
140 substitute at that position. Further, we identify an ExbD-specific cyclic peptide that, when added to *E.*
141 *coli* exogenously, prevents binding of ExbD to its protein partners and inhibits the TonB system.

142 **RESULTS**

143

144 *The negative charge and location of Asp25 in the ExbD transmembrane domain are indispensable for*

145 *TonB system function*

146

147 The ExbD transmembrane domain is predicted to consist of residues 23-43 (20). The similarity

148 of the ExbD transmembrane domain to those of paralogues TolR and MotB suggested that ExbD D25

149 (D23 in TolR and D32 in MotB) might be important (48, 49). To investigate that possibility, Cys

150 substitutions were engineered individually at all predicted ExbD transmembrane domain residues from

151 23 to 43 on plasmid pKP999 under a propionate-inducible promoter [(29); see Fig. 3A for the primary

152 amino acid sequence]. Individual Cys substitution mutants were expressed at chromosomal levels in

153 strain RA1045 (Δ*exbD,* Δ*tolQR*), where the paralogues TolQR were also removed and could no longer

154 serve as a source of limited but detectable TonB system activity (28, 53-55). All Cys-substituted ExbD

155 mutant proteins were proteolytically stable and, excluding the slower migration of ExbD D25C and

156 ExbD P39C, migrated at the same position as wild type ExbD in immunoblots (Fig. 4, lower panel). The

157 slower migration of D25C appeared to reflect the loss of the Asp residue since D25N and D25A

158 substitutions also decrease ExbD mobility in sodium dodecyl sulfate (SDS) polyacrylamide gel

159 electrophoresis (data not shown). A case where ExbD migrates more slowly because it appears to be

160 chemically modified is considered below. Except for ExbD D25C, which was insensitive (tolerant) to

161 all agents tested, the Cys substitutions of residues 23-43 supported sensitivity to colicin B, Ia, M and

162 bacteriophage ϕ80 (Table 1). These TonB-system assays are the most sensitive, detecting the activity of

163 as little as one TonB per bacterial cell (56).

164 To further test the importance of Asp25 in ExbD, all 19 other amino acids were substituted at

165 that position. The conservative replacement ExbD D25E retained 5-10% wildtype activity in iron

166 transport assays, which are the most discriminative of the TonB system assays, while the remaining 18

167 substitutions at Asp25 were completely insensitive in colicin and phage sensitivity assays, indicating
168 that they supported no TonB system activity (56).
169 Relocation of His20 in the TonB transmembrane domain from position 20 to a higher turn of the
170 spiral at position 24 supports detectable but decreased colicin and phage sensitivity (26). To test the
171 importance of its position within the ExbD transmembrane domain, Asp25 was relocated to all other
172 positions in the ExbD transmembrane domain from position 23 to 43 on a plasmid template where
173 Asp25 was mutated to Ala. In contrast to the situation with TonB His20, all the ExbD Asp25 relocation
174 mutants were completely insensitive to colicin and phage. Taken together these results indicated that the
175 negative charge and location of ExbD Asp25 within the transmembrane domain were essential for its
176 activity.
177
178 *Sequence comparisons with ExbD paralogues TolR and MotB*
179
180 We had previously used the TOPCONS program to predict ExbB, TolQ, MotA and PomA
181 transmembrane domain boundaries (57). In that study, TOPCONS provided a prediction that was
182 congruent with a number of conserved residues within their transmembrane domains and led to a
183 redefinition of boundaries for the last two TMDs of each protein (27). Here TOPCONS analysis of the
184 individual protein sequences was less helpful, potentially due to divergence in the function of these
185 proteins compared to ExbB and its paralogues.
186 The invariant and essential Asp residue found in ExbD, TolR, MotB and PomB transmembrane
187 domains did not align well using TOPCONS: the majority of homologies between the paralogous
188 proteins ExbD and TolR were missed; congruence between ExbD and MotB Cys substitutions that
189 formed high levels of disulfide-linked complexes were not optimized; and homologies between MotB
190 and PomB, both of which play similar roles in flagellar rotation, were not optimized (Fig 3A). Because
191 ExbD appears to interact with the last two transmembrane domains of ExbB, it seemed likely that

192 TolR/MotB/PomB proteins should interact similarly with TolQ/MotA/PomA (27). This appeared to be
193 the case since the inconsistencies generated by the TOPCONS analysis were resolved when the
194 transmembrane domains were aligned using the invariant Asp residues (Fig. 3B). Notably, the ExbD
195 Cys substitutions that homodimerized most efficiently (described below) were now aligned with the
196 MotB substitutions that homodimerized most efficiently.
197
198 *ExbD homodimerizes through residues 23-63* in vivo.
199
200 We had previously identified residues in the region of residues 92-121 through which ExbD
201 periplasmic domains homodimerized *in vivo* (36). To study the ability of the ExbD transmembrane
202 domain to support homodimerization in the absence of its periplasmic domain, the DNA encoding ExbD
203 residues V23-P63 was cloned into the TOXCAT vector, pccKan (58). The cloned region included the
204 predicted ExbD transmembrane domain [(residues 23-43); (20)] and a subsequent unstructured domain
205 involved in signal transduction [(residues 44-63) (59, 60)].
206 As part of the TOXCAT fusion protein, if residues 23-63 homodimerized they would mediate
207 concomitant homodimerization of the amino terminal, cytoplasmically localized ToxR domain, thus
208 activating the chloramphenicol acetyl transferase gene (CAT) and supporting increased resistance to
209 chloramphenicol (CAM) compared to controls where the transmembrane domain does not
210 homodimerize (GlpA compared to GlpA G83I in the TOXCAT vector). Activity of carboxy terminally
211 fused periplasmic maltose binding protein (MBP) would serve as a control to demonstrate that the
212 inserted ExbD residues had translocated MBP to the periplasmic space.
213 To test homodimerization by ExbD residues 23-63, plasmid vector pccKan, plasmid pccGlpA,
214 plasmid pccGlpA G83I and pKP523 [pccExbD (*toxR-exbD*$_{23\text{-}63}$*-malE*)] were transformed into strain
215 NT326 [*araD*139, Δ(*argF-lac*)$_{U169}$, Δ*malE444, recA*1, *thi*, *strR* (61)] and KP1448 (NT326, *exbB*::Tn*10*).
216 Resistance to various concentrations of CAM, from 34 μg/ml to 1.0 mg/ml was measured by growth on

217 plates. In NT326, both GlpA-TOXCAT and $ExbD_{23-63}$-TOXCAT supported strong growth on 125 $\mu$g/ml
218 CAM and poor growth at 500 $\mu$g/ml. The GlpAG83I-TOXCAT mutant control supported poor growth
219 at 125 $\mu$g/ml and no growth at 500 $\mu$g/ml (Table 2). In KP1448, where competition by wild-type ExbD
220 transmembrane domains was eliminated, $ExbD_{23-63}$-TOXCAT and GlpA-TOXCAT again supported
221 equally robust growth on 0.125 $\mu$g/ml CAM. Again, there was little growth of the negative control,
222 GlpA G83I-TOXCAT, at that concentration (Table 2). The three TOX-CAT constructs containing
223 GlpA, GlpA G83I, or $ExbD_{23-63}$ residues equally supported growth with maltose as sole carbon source
224 and had equivalent levels of protein present on anti-MBP immunoblots (data not shown), indicating that
225 they were equally expressed and exported to the cytoplasmic membrane. We concluded that ExbD
226 residues 23-63, which included the predicted transmembrane domain, had an intrinsic ability to form
227 homodimers *in vivo* in both the presence and absence of ExbB.
228
229 *Identification of a face through which ExbD transmembrane domains homodimerize*
230
231 To determine if homodimers formed through the predicted ExbD transmembrane domain,
232 disulfide-mediated homodimerization of ExbD Cys-substitutions at residues 23-43 expressed at
233 chromosomal levels was evaluated using iodine ($I_2$) catalysis, a technique previously used to study
234 homodimerization of TolR and MotB transmembrane domains (46, 47). In Fig. 4A, several of the Cys
235 substitutions resulted in bands on non-reducing anti-ExbD immunoblots that, at ~ 31 kDa, were twice
236 the mass of monomeric ExbD (~15 kDa) (45). The ~ 31 kDa complex was absent from an ExbD
237 deletion strain (RA1045, Δ*exbD*, Δ*tolQR*) and from wild-type (Cys-less) ExbD samples (WT and
238 pExbD), indicating that it represented a disulfide-linked ExbD homodimer. The efficiency of dimer
239 formation varied with the position of the Cys residue. The most abundant dimers were formed by
240 residues I24C, M27C, F34C, with a periodicity of ~3-4 amino acids (and a gap at 30-31C), consistent

241 with an α-helical arrangement of each ExbD transmembrane domain and suggesting that they
242 homodimerize through one face (Fig. 4B).
243 Similar results are seen for paralogues MotB and TolQ (46, 47). TolR, MotB, and as we
244 demonstrated above, ExbD, all carry a functionally important Asp residue in their single transmembrane
245 domain at positions 23, 32, and 25 respectively (47, 49). Further similarity was demonstrated by ExbD
246 I24C, which existed entirely in homodimeric form, with ExbD D25C existing mostly in monomeric
247 form in this assay (Fig. 4A). A similar relationship was seen with corresponding MotB transmembrane
248 domain Cys substitutions at A31C and D32C (46), suggesting that the transmembrane domains
249 homodimerize similarly. In contrast to a predicted α-helical configuration, each of the ExbD Cys
250 substitutions from L40C- V43C formed homodimers with little to no monomer. It was not clear if the $I_2$
251 oxidant or ExbB was needed to form any of the complexes.
252 Although all the ExbD mutants were expressed at near chromosomal levels as determined by
253 reducing SDS polyacrylamide gel electrophoresis (Fig. 4A, lower), there was differential antibody
254 detection of both monomers and homodimers from the same samples immunoblotted under non-
255 reducing conditions (Fig. 4A, upper). For example, V26C monomer was detected at just slightly less
256 than wild-type monomer ExbD levels on the reducing immunoblot (Fig. 4A, lower) but was much more
257 strongly detected compared to the wild-type ExbD on the non-reducing immunoblot (Fig. 4A, upper)
258 and did not form homodimers. In contrast, ExbD P39C appeared to be undetectable on the non-reducing
259 immunoblot and was present at wild-type chromosomal levels on the reducing immunoblot. The
260 differential antibody detection suggested that there was structural variation among ExbD Cys
261 substitutions under non-reducing conditions, even in the presence of SDS.
262
263 *ExbD transmembrane domain Cys substitutions 23-39 require oxidant for homodimerization whereas*
264 *Cys residues at 40-43 do not.*
265

266 To determine if oxidant was required for transmembrane domain homodimerization, the
267 experiment in Fig. 4A was repeated but without the use of $I_2$ (Fig. 5). Near the cytoplasmic side of the
268 predicted transmembrane domain, I24C spontaneously formed only modest levels of homodimers in
269 contrast to the high level I24C formed when $I_2$ was present, thus placing it within the transmembrane
270 domain. In contrast, ExbD F23C appeared to be on the transmembrane domain boundary because it
271 formed similarly low levels of homodimers with and without $I_2$ (compare Figs. 4A and 5). Consistent
272 with an apparent transmembrane domain location, none of the residues from D25C through P39C
273 spontaneously formed significant levels of homodimers in the absence of $I_2$.
274 In contrast, residues from ExbD L40C- V43C each spontaneously formed high levels of
275 homodimers in the absence of $I_2$, suggesting they were not part of the transmembrane α-helix and likely
276 constituted a region of intrinsic disorder (compare Figs. 4A and 5).
277
278 *Trapping ExbD homodimers through T42C or V43C largely inactivates the TonB system.*
279
280 Because ExbD T42C and V43C resulted in almost 100% homodimer formation in the absence of
281 $I_2$ oxidant in Fig. 5, it was possible to determine whether dynamic movement of those residues was
282 required for TonB system activity. We assayed the ability of plasmids expressing each variant to
283 support TonB-dependent iron transport with or without the reducing agent dithiothreitol (DTT) and
284 immunoblotted those same cultures to determine relative steady state levels of monomer and
285 homodimer. As seen previously, both ExbD T42C and V43C were nearly 100% homodimerized in the
286 absence of DTT (Fig. 6A, upper panel). All ExbD Cys substitutions were expressed at chromosomally
287 encoded levels (Fig. 6A, lower panel).
288 In Fig. 6B, DTT had an inhibitory effect, decreasing the initial transport rate of the wild-type
289 control to 77% of the rate seen in the absence of DTT. We compensated for the fact that DTT was
290 somewhat inhibitory to wild-type transport by calculating the mutant transport rates as percentiles of the

291 wild-type transport rates. The effect of DTT on the previously trapped inactive homodimers of
292 ExbDT42C and ExbDV43C, was to release them as monomers, thus restoring activity (Fig 6A, upper
293 panel). Transport supported by trapped ExbD V43C was restored from 9% of wild-type -DTT to 89% of
294 wild-type +DTT (Fig. 6C; Table 3). Similarly, DTT restored transport supported by ExbD T42C from
295 23% of wild-type -DTT to 77% of wild-type +DTT. These results indicated that inactivity of the
296 disulfide-linked homodimers was due to restriction of required conformational changes rather than the
297 inability of Cys to functionally replace Val or Thr. The results were not contradictory with the spot titer
298 data from Table 1 where strains expressing ExbD T42C or V43C were sensitive to colicins and phage
299 due to the presence of residual monomer. The highly sensitive colicin spot titers detect activity from as
300 little as 1 molecule of active TonB (56, 62).
301 The results were consistent with the existence of an energy transduction cycle where, if ExbD is
302 trapped in a homodimeric configuration such as Stage I or II, it cannot progress through the cycle (Fig.
303 2). Residues L40-V43 are contiguous with a region of intrinsic disorder from 44-63 that dynamically
304 interacts with a second ExbD, with ExbB and with TonB *in vivo* (35, 59, 60).
305
306 *ExbD T42C appears to undergo increased modification in the absence of ExbB.*
307
308 Data presented in Fig. 6A (lower panel) suggested that monomeric ExbD T42C might be
309 chemically modified, because while a majority of ExbD T42C was found migrating at the same position
310 as wild-type ExbD on immunoblots of reducing SDS polyacrylamide gels, a smaller amount appeared to
311 migrate at a slightly higher apparent mass. To determine the parameters that affected the potential
312 modification, the migration of ExbD T42C was evaluated on immunoblots of strains lacking ExbD, both
313 ExbB and ExbD, or both ExbD and TonB (Fig. 7). As seen in Fig. 6A, both unmodified and modified
314 ExbD T42C were again observed, with ~ 2/3 in the unmodified form (Fig. 7, lane 6). The absence of
315 ExbB (and paralogue TolQ) converted all the ExbD T42C into the higher mass form (Fig. 7, lane 7). In

316 the absence of TonB, the relative proportion of the two forms was reversed relative to the wild-type
317 situation, with ~2/3 of the ExbD T42C found at the position of the higher mass form (Fig. 7, lane 8). It
318 is not clear whether the modification has any *in vivo* relevance for the mechanism of TonB-dependent
319 energy transduction. At the very least it provides evidence of *in vivo* interactions between ExbD and
320 ExbB. It is included here for future researchers. Apparent chemical modification of full-length wild-
321 type ExbD also occurs when an inhibitory ExbD peptide (residues 44-63) is expressed endogenously,
322 resulting in the appearance of a higher mass ExbD species (63).
323
324 *Transmembrane domain Cys residues require ExbB for homodimerization whereas those of the*
325 *potentially disordered domain do not.*
326
327 Because the $ExbD_{23-63}$-TOXCAT fusion protein homodimerized in the absence of ExbB, we
328 tested the role of ExbB in ExbD homodimerization through its transmembrane domain by expressing
329 each of the Cys-substituted proteins in RA1017 (*ΔexbBD, ΔtolQRA*). Unexpectedly, in light of the
330 TOXCAT results, the absence of ExbB prevented the previously detected $I_2$-dependent disulfide-linked
331 dimerization through ExbD substitutions F23C-P39C, even though $I_2$ was present (compare Figs. 4 and
332 8). This finding notably contrasts with MotB transmembrane domain homodimer formation through
333 engineered Cys substitutions, which does not depend on MotA (46).
334 In contrast, even without ExbB, residues contiguous to the transmembrane domain, L40C, A41C
335 and V43C, formed homodimers, with V43C again achieving nearly 100% dimer formation (Fig. 8). The
336 results suggested that because two ExbD molecules were in sufficient proximity to homodimerize
337 through an adjacent region of likely intrinsic disorder, it seemed likely that the transmembrane domains
338 also interacted, but in a way not captured by disulfide cross-linking in the presence of $I_2$. In addition,
339 these results suggested that the source of ExbB-independent homodimerization by the $ExbD_{23-63}$-
340 TOXCAT fusion protein resided in the disordered domain.

341 In the absence of ExbB, ExbD T42C formed essentially no homodimers, suggesting either that
342 the Cys substitution was the site of chemical modification observed in Fig. 7 or that without ExbB, two
343 T42C residues were no longer in proximity for disulfide formation. The latter explanation was excluded
344 because A41C and V43C on either side of T42C formed disulfide-linked homodimers (Fig. 8). We
345 therefore conclude that chemical modification occurred at ExbD T42C in the absence of ExbB.
346
347 In vivo *photo-cross-linking suggests that ExbD transmembrane domains rotate relative to each other*
348 *and relative to ExbB*.
349
350 Disulfide linkage of ExbD Cys substitutions trapped transmembrane domains in a static
351 homodimeric state where the most abundant cross-linking occurred between residues on an apparently
352 helical face (Fig. 4A). Nonetheless, there was minor cross-linking that occurred through two ExbD
353 D25C residues on an opposing face of that helix, consistent with the idea that the transmembrane
354 domain helices might rotate relative to one another. Because the homodimerized transmembrane
355 domains of TolR, which can functionally substitute for ExbD in the TonB system, rotate relative to one
356 another *in vivo* (47), we wanted to determine if that was also true for ExbD. Rather than disulfide cross-
357 linking, we used *in vivo* photo-cross-linking by the reagent *p*-benzoyl-l-phenylalanine (pBpa), which
358 inserted efficiently at each amber codon for T21, V23, I24, D25, M27, V29, I32, D34, M35, and A37
359 (Fig. 9A, lower panel; monomeric ExbD).
360 In the presence of ultraviolet light, the ExbD pBpa monomers were pulled into three higher mass
361 complexes on immunoblots: ExbD homodimers and two ExbD-ExbB complexes with different apparent
362 masses (termed "upper" and "lower") characterized previously [Fig. 9A, upper panel (59)]. Each of the
363 ExbD pBpa substitutions formed homodimers and to different extents. Abundant homodimers were
364 formed by I24pBpa and F34pBpa, two sites that, as Cys substitutions, were part of the proposed α-
365 helical dimerization face (compare Figs. 4 and 9A). In addition, equally abundant homodimers were

366 formed by D25pBpa and V29pBpa, two residues on the opposite side of that face (Fig. 9 A and B).
367 Taken together, the results indicated that each of the transmembrane domain pBpa substitutions had
368 access to a second, homodimerized ExbD, most likely through its transmembrane domain. To achieve
369 contacts through residues on opposite faces of the α-helix, the transmembrane domain must have moved
370 relative to a second ExbD, possibly by rotation. Because all the transmembrane domain ExbD pBpa
371 substitutions formed complexes with ExbB (upper), they may have rotated relative to ExbB as well. Half
372 of the pBpa-substituted ExbDs also formed complexes with ExbB (lower) (Fig. 9A).
373
374 *ExbD L132 plays only a structural role in the TonB system.*
375
376 The Braun lab isolated the first inactive missense mutation in the ExbD periplasmic domain,
377 L132Q (43). It stalls TonB at Stage I of the energy transduction cycle and, unlike wild-type ExbD, does
378 not formaldehyde cross-link to TonB *in vivo* [Fig. 2; (42)]. Deletion of the last 10 residues of ExbD
379 (Δ132-141) render it inactive, possibly due to the loss of L132 (35). To determine if L132 was an
380 essential residue like D25 in the ExbD transmembrane domain, we engineered substitutions of all 19
381 amino acid residues at position L132 in pKP999. The relative activity of the ExbD variants was
382 assessed by ability to complement the RA1045 Δ*exbD* mutation in a growth assay in M9 minimal
383 medium, where iron is limiting and only the TonB+ strains grow. As shown in Table 4, L132 is not an
384 essential residue since it could be substituted with Cys, Val, Ile, Met, Phe, and Trp and still retain full
385 activity. It seems likely that the Gln substitution in L132Q inactivated the TonB system by preventing
386 ExbD interaction with TonB through steric hindrance.
387
388 *A cyclic peptide derived from ExbD inhibits TonB system activity and prevents formaldehyde-specific*
389 *TonB-ExbB and TonB-ExbD cross-linked complexes* in vivo
390

391 The TonB system is a virulence factor for many Gram-negative bacteria (9). The periplasmic
392 domains of two key proteins in the system, ExbD and TonB, and their required interaction for
393 subsequent active transport through outer membrane TBDTs make it an appealing target for novel
394 antibiotic development. In general, antibiotics that inhibit periplasmic activities need possess only the
395 hydrophilic chemical characteristics that allow diffusion through outer membrane porins to access their
396 targets, a distinct advantage over those that must additionally cross the hydrophobic cytoplasmic
397 membrane (64).
398 Periplasmic ExbD residues 44-63 are disordered and thus a likely site for interaction with other
399 proteins (60, 65). We began to identify inhibitory regions of ExbD using endogenous secretion of
400 promising small peptides into the periplasmic space. Secretion of a disordered region peptide (residues
401 44-63) inhibits TonB-dependent iron transport by inhibiting an essential ExbD-TonB interaction, thus
402 establishing a proof of principle (63).
403 In this work we targeted interactions between ExbD and TonB periplasmic domains using
404 exogenously added peptides. Cyclic rather than linear peptides were chosen to decrease the likelihood
405 of proteolytic degradation by periplasmic proteases. None of the peptides contained cleavage sites for
406 the outer membrane protein, OmpT (66). Inhibitory cyclic peptides were designed based on three
407 regions of ExbD that are essential for TonB system activity *in vivo* [Fig. 10; (35, 36, 44)]: Region 1,
408 residues 44-63 from the ExbD periplasmic disordered region adjacent to the transmembrane domain, an
409 essential motif required for the ExbD-TonB PMF-dependent interaction (59); Region 2, residues 92-121
410 that are required for *in vivo* formaldehyde cross-linking of all known ExbD complexes (ExbD-ExbD,
411 ExbD-TonB, and ExbD-ExbB) (35); and Region 3, the region surrounding ExbD residue, L132, where a
412 single substitution, L132Q, completely abolishes activity (43).
413 The cyclic peptides from Region 1 of ExbD were the motifs V-K-V-N-L-P and V-K-V-N-L-P-A,
414 where the latter contained a carboxy terminal alanine to provide more conformational flexibility. For

415 Region 3, the sequence of ExbD residues 129-134 (K-I-G-$L_{132}$-V-G) was chosen along with the
416 corresponding mutant peptide representing ExbD L132Q (K-I-G-$Q_{132}$-V-G).
417 Because the larger ExbD Region 2 (residues 92-121) lacks specifically identified targets and has
418 extensive conservation of residues among most of the Gram-negative ESKAPE pathogens responsible
419 for some of the most deadly acquired hospital infections [(Fig. 10), (67)], studies of protein-protein
420 interactions were used to further guide the choice of residues. The sequence I-F-F-R-A-D (residues 102-
421 107) was deemed likely to be a site of ExbD-ExbD interaction because it contains a concentration of
422 hydrophobic residues (IFFA), which are commonly found at protein-interaction interfaces (68). In
423 addition, three of the top five "hotspot" amino acid preferences which contribute the most binding
424 energy in a protein interaction, were present within the semi-conserved sequence region shown in Fig.
425 10 [Ile, Arg, and Asp (69)]. Asp 207 was excluded from the cyclic peptide to facilitate transit through
426 porins in the outer membrane which have a size limit of ~ 600 da (70).
427 --*Cyc-IFFRA inhibits TonB-dependent activity*. To eliminate potential efflux of peptides out of
428 the periplasm, strain SH03 (W3110, *tolC*::Tn*10*) was used (71). Initial rates of TonB-dependent $^{55}$Fe-
429 ferrichrome transport were determined in the presence of cyclic (cyc) peptides cyc-VKVNLP and cyc-
430 VKVNLPA from Region 1; cyc-IFFRA from Region 2; cyc-KIGLVG, and cyc-KIGQVG from Region
431 3 (Fig. 11). In the presence of cyc-IFFRA, the $^{55}$Fe-ferrichrome initial transport rate was reduced to
432 ~30% of the SH03 + DMSO control, indicating that it interfered with TonB system activity. Cyc-
433 VKVNLP, cyc-VKVNLPA, cyc-KIGLVG, and cyc-KIGQVG had no effect on $^{55}$Fe- ferrichrome
434 transport. These results suggested that either the peptides were not inhibitory or that they did not
435 efficiently enter the cells. In any case the L132Q mutation results were uninterpretable since the Region
436 3 peptide encoding the wild-type version had no detectable effect.
437 --*Cyc-IFFRA inhibits formation of TonB-ExbD and, surprisingly, TonB-ExbB complexes* in vivo.
438 Stage III of the TonB energy transduction cycle is characterized by the PMF-dependent formation of
439 formaldehyde cross-linked ExbD-TonB complexes (Fig. 2). Cys substitutions K97C and T109C on

440 either side of the Region 2 peptide-derived sequence IFFRA capture multiple interactions with Cys
441 substitutions in the periplasmic TonB carboxy terminus *in vivo*, and formation of those disulfides is
442 significantly reduced or nonexistent in the PMF-unresponsive mutant, ExbD D25N (44). Taken together
443 these results suggested that the inhibitory effect of cyc-IFFRA could be due to inhibition of Stage III of
444 the energy transduction cycle. To test that hypothesis, strain SH03 was treated with formaldehyde in the
445 presence of the five cyclic peptides evaluated in Fig. 11 and processed for immunoblotting with both
446 anti-ExbD and anti-TonB antibodies (Fig. 12).

447 Consistent with its inhibition of iron transport in Fig. 11, the Region 2 cyc-IFFRA peptide
448 prevented the Stage III TonB-ExbD complex detected with both anti-TonB antibody (Fig. 12A) and
449 anti-ExbD antibody (Fig. 12B). It also unexpectedly decreased formation of TonB-ExbB complexes
450 compared to the control (SH03 + DMSO), but not TonB-Lpp, TonB-OmpA or TonB-FepA complexes.
451 Formaldehyde cross-linking of TonB with Lpp and OmpA appear to be off-pathway contacts made by
452 unenergized TonB since a double *lpp, ompA* mutant has only slightly reduced iron transport (14). The
453 FepA complex likewise represents an inactive TonB-FepA complex which occurs with unenergized
454 TonB (72). The cyc-IFFRA peptide had no effect on ExbD homodimer or ExbD-ExbB heterodimer
455 formation.

456 Inhibition of the TonB-ExbB complex by a cyclic peptide corresponding to a distal periplasmic
457 region of ExbD suggested that this region of ExbD played a role in assembly or conformation of the
458 TonB-ExbB interaction *in vivo*. While monomeric formaldehyde is a probe for close contacts (73), the
459 absence of a formaldehyde-cross-linked complex only means that the formaldehyde-cross-linkable
460 residues have moved out of correct apposition--due either to dissolution of the complex or to a change in
461 conformation of one or more proteins within the complex.

462 The cyc-VKVNLPA peptide from Region 1 appeared to formaldehyde cross-link to ExbD
463 monomer (labeled "?") and disrupt ExbD homodimer cross-linking (Fig. 12B), consistent with our
464 identification of ExbD homodimerization through Region 1 residues in full-length ExbD (59).

465 Monomeric formaldehyde inserts a $CH_2$ group between two reactive residues (K, Y, H, C ⋙ R, W)
466 (74). It seems likely that cyc-VKVNLPA formaldehyde cross-linked to ExbD monomer through its Lys
467 residue. None of the other peptides contained strongly cross-linkable residues, which explains why
468 binding to ExbD monomer was not detected with the inhibitory cyc-IFFRA peptide from Region 2. If
469 cyc-VKVNLPA did cross-link to ExbD monomer, it means that it was able to penetrate the outer
470 membrane, even though it was the largest of the peptides. This result suggested how sensitive
471 translocation across the outer membrane, presumably via porin proteins, was to overall conformation
472 because the smaller version of the same peptide that also contained a cross-linkable Lys residue
473 apparently did not enter the periplasm. Alternatively, it did, but could not bind to ExbD. Because cyc-
474 VKVNLPA did not affect the iron transport rate in Fig. 11, it was not a candidate to be a TonB system
475 inhibitor. Cyc-IFFRA, however, showed promise.

476 **DISCUSSION**

477

478 Outer membrane active transporters of Gram-negative bacteria, including ESKAPE pathogens,
479 are powered by the TonB-system (75), which is one of three systems in *E. coli* K12 that each use two
480 similar cytoplasmic membrane proteins and the PMF to power cell envelope events: ExbB and ExbD of
481 the TonB system energize active transport across the outer membrane (76); TolQ and TolR power
482 proper outer membrane invagination (77); MotA and MotB act as stators for flagellar rotation (78). Of
483 the three systems, the TonB system is the least complex so far with ExbB/D and TonB located in the
484 cytoplasmic membrane and a variety of TBDTs in the outer membrane (Fig. 1), although there is
485 evidence for additional mystery proteins (79, 80). What they all have in common are residue similarities
486 in the last two transmembrane domains of ExbB/TolQ/MotA and an invariant Asp residue in
487 approximately the same position in the single transmembrane domain of ExbD/TolR/MotB. Other than
488 similarities among their transmembrane domains, the remaining residues most likely account for their
489 disparate functions. The overall mechanism of TonB-mediated energy transduction remains a mystery.
490 Results from the also-mysterious Mot and Tol systems provide informative comparisons.

491 *In vivo* studies of the paralogue MotB transmembrane domain demonstrate the importance of
492 Asp32 (D25 of ExbD; D23 of TolR) to flagellar rotation, where out of 15 substitutions only the
493 conservative replacement D32E shows a slight amount of activity (49). MotB (308 residues) forms
494 homodimers through a face on its single α-helical transmembrane domain (46, 81). MotB also binds to
495 peptidoglycan through residues ~ 209-227, a logical function for a flagellar rotation stator (82, 83). The
496 need for a "plug" (MotB residues 52-65, C-terminal to the transmembrane domain) is explained if
497 unassembled MotA/B complexes leak protons until they are assembled in the flagellar motor (84).

498 *In vivo* studies on paralogue TolR (142 residues in length) show that two TolR transmembrane
499 domains homodimerize in a pattern similar to the MotB transmembrane domains (Fig. 3B). Like MotB,
500 TolR has a conserved Asp residue in its transmembrane domain that is inactivated by the D23R

501 substitution, while the conservative D23E substitution retains lower but detectable activity (48). ExbB/D
502 and TolQ/R are the most closely related paralogues and can in fact substitute (~ 10%) for one another in
503 their respective interactions with either non-cognate TonB or Tol-Pal proteins (45, 53-55, 85). Cys
504 substitution Y117C in the periplasmic carboxy terminus traps TolR such that it cannot undergo needed
505 conformational transformations (86). Similarly, disulfide-linked homodimers through the corresponding
506 residue in ExbD (Y112C) are inactive (36). Both results speak to the dynamic nature of their respective
507 periplasmic domain interactions.

508 Unlike the MotB transmembrane domains that apparently retain a static relationship and thereby
509 support binding of its periplasmic domain to peptidoglycan, homodimeric TolR transmembrane domains
510 appear to rotate relative to one another. Cys substitutions on opposite sides of the transmembrane
511 domain helix [L22 and V24 (corresponding to ExbD I24 and V26, Fig. 3B),] trap TolR as disulfide-
512 linked homodimers that inactivate the Tol system. Addition of the reducing agent DTT reduces the
513 disulfide bond and restores activity (47). This requirement for movement raises a question whether the
514 TolR periplasmic domain binds to peptidoglycan *in vivo*. Consistent with that, TolR is less than half the
515 length of MotB, seemingly making it less likely to access the peptidoglycan. In addition, TolR also does
516 not have an identifiable plug. In a contrasting view, TolR is hypothesized to reach the peptidoglycan as
517 a disordered protein (87). Cryptic peptidoglycan binding is observed for a truncated TolR periplasmic
518 domain, but it is not clear how the binding affinity compares to that of canonical OmpA peptidoglycan
519 binding (88).

520

521 *The ExbD transmembrane domain*. At 141 residues, ExbD is essentially the same length as
522 TolR (45). Braun et al. were the first to show that ExbD D25N is inactive (43). Our *in vivo* studies
523 described here on the predicted ExbD transmembrane domain (residues 23-43) were late to the party but
524 were somewhat more thorough from a mutagenic point of view. They first of all indicated that, like the

525 MotB and TolR transmembrane domains, the ExbD transmembrane domain homdimerized in an α-
526 helical configuration.

527 All residues in the ExbD transmembrane domain except Asp25 could be substituted with Cys
528 and retain function in colicin and phage sensitivity assays. Replacement by none of the remaining 19
529 amino acids at residue 25 except the conservative replacement D25E supported any activity, thus
530 aligning well with the importance of the transmembrane domain Asp in MotB and TolR (48, 49). For
531 the first time, alternative positions for Asp25 within the transmembrane domain were assessed, showing
532 that ExbD Asp25 did not function at any other position within the transmembrane domain. Because
533 participation of the TonB and ExbB transmembrane domains in PMF-responsiveness is ruled out, it
534 appears that in the TonB system PMF is engaged solely through ExbD Asp25 (26, 27). Consistent with
535 that, progression to Stage III in the energy transduction cycle is prevented either by the protonophore
536 CCCP (carbonyl cyanide *m*-chlorophenyl hydrazone) that collapses PMF or by the unresponsive *exbD*
537 D25N mutation [Fig. 2; (29, 42)].

538

539 *Two different domains in the ExbD amino terminal region*. Residues 23-43 were originally
540 proposed to constitute the ExbD transmembrane domain (20). Our results suggested instead that the
541 functional boundaries of the ExbD transmembrane domain could be revised to extend only from ExbD
542 F23 to P39. A set of three ExbD Cys substitutions in this region appeared to represent an α-helical
543 configuration, requiring both oxidant and the presence of ExbB to form disulfide-linked homodimers
544 through those residues. This revision somewhat positions the ExbD transmembrane domain between
545 two prolines at residues 22 and 39, that are conserved in TolR but not MotB (Fig. 3).

546 In contrast, each sequential residue from L40C through V43C homodimerized strongly without
547 the requirement for either added oxidant or ExbB, suggesting that they constituted an intrinsically
548 disordered domain. [ExbD T42C did not homodimerize in the absence of ExbB because it appeared to
549 be chemically modified.] Thus, ExbD residues L40-V43 appeared to initiate the previously identified

550 intrinsically disordered region of ExbD that terminates with residue 63, homodimerizes, and contains the
551 conserved motif V45-V47-L49-P50 that is required for signal transduction of PMF to the TonB
552 periplasmic domain (59, 60).

553 The $ExbD_{23-63}$-TOXCAT fusion protein, where none of the residues was Cys-substituted,
554 homodimerized either through ExbD transmembrane domain residues (residues 23-39) or an apparently
555 disordered region (residues 40-63), or both. That result ruled out a requirement for participation of the
556 Dsb system in $ExbD_{23-63}$ homodimerization. The $ExbD_{23-63}$ -TOXCAT fusion protein homodimerization
557 did not require ExbB, indicating an intrinsic ability to homodimerize that was consistent with previous
558 studies identifying homodimerization through residues 44-56 using *in vivo* photo-cross-linking (59) and
559 disulfide-linked homodimerization of ExbD through Cys substitutions in its periplasmic domain
560 (residues 92-121) that also does not require ExbB *in vivo* (36). It thus appeared that both disordered and
561 ordered regions of the ExbD periplasmic domain homodimerized independently of ExbB and it is likely
562 that the observed homodimerization of $ExbD_{23-63}$ -TOXCAT both in the presence and absence of ExbB
563 was due to the presence of the disordered region and not the transmembrane domain. If the entire
564 periplasmic domain of ExbD homodimerizes independently of ExbB, perhaps it might initiate formation
565 of ExbD transmembrane domain homodimers rather than vice versa.

566

567 *Required motion of the ExbD transmembrane domains*. Because L40C-V43C homodimerized in
568 the absence of ExbB, it suggested that the ExbD residues 23C-39C were likely also homodimerized due
569 to their proximity in the absence of ExbB, but without formation of disulfide-linked homodimers.
570 Combined, these results suggested that the ExbD transmembrane domains had the capacity to
571 homodimerize in two different configurations *in vivo* which could be consistent with a requirement for
572 motion. The importance of motion was confirmed when spontaneously disulfide-linked Cys
573 substitutions at positions T42 and V43 inactivated TonB-dependent transport and reduction of the

574 disulfides reactivated it. These results mirrored similar approaches showing that TolR transmembrane
575 domains rotate relative to one another (47).
576 Results from *in vivo* photo-cross-linking studies suggested that the motion could be rotation
577 because sites on all faces of the ExbD transmembrane domain participated in formation of homodimers.
578 Consistent with that idea, *in vivo* photo-cross-linking also showed that all sites investigated in the ExbD
579 transmembrane domain formed photo-cross-linked complexes with ExbB.
580 Thus, two different techniques have now identified the likely rotation of ExbD/TolR
581 transmembrane domain homodimers relative to one another *in vivo*. By assessing disulfide-linked
582 homodimers, Celia et al. also suggested that the ExbD transmembrane helices rotated with respect to one
583 another (89).
584
585 *Results in the context of recent subcomplex cryo-EM structures*. The recent cryo-EM structures
586 of ExbB/D and MotA/B from several species show them to be asymmetric subcomplexes of 5
587 ExbB/MotA and 2 ExbD/MotB (51, 52, 89). The congruence of the proposed structures is striking,
588 especially since it is seen across different species and with the GldL/M proteins involved in gliding
589 motility of *Flavobacterium johnsoniae* (90). Authors of the MotA/B cryo-EM papers suggest that
590 MotA rotates around MotB homodimer, held static by interaction with peptidoglycan (51, 52). Hennell-
591 James et al. suggests that the GldL pentamer rotates relative to the GldM homodimer (like MotB) (90).
592 It has been suggested that these admittedly beautiful structures provide the key to the mechanism of the
593 protein complexes that all use PMF for energy (91) and that ExbB/D follows the same mechanism as
594 MotA/B (51).
595 An argument can be made for the validity of the MotAB structure because the first
596 transmembrane domain of MotA, which has four rather than three transmembrane domains like ExbB
597 and TolQ, stands in for their respective TonB/TolA transmembrane domains, thus obviating concerns
598 that TonB is not part of the ExbB/D cryo-EM structures and providing reassurance for the other

599 structures that, because they all exhibit the same 5:2 asymmetric architecture, they accurately reflect the
600 *in vivo* state of the complexes. Nonetheless, there is still a need to understand how and where
601 TonB/TolA fit into ExbB,TolQ/ExbD,TolR complexes and to address the cellular ratios of 7
602 ExbB/TolQ:4 ExbD/TolR:1TonB/TolA (11, 48, 92).

603 More remains to be discovered about the mechanism of these proteins. As Deme et al. states "No
604 ion permeation across the bilayer was seen in any simulation, supporting the idea that the complexes
605 currently seen will require rearrangement for activity." (51). Celia et al. likewise did not see a channel
606 in ExbB5/D2 through which a proton could be translocated and suggest that structural plasticity is likely
607 important (89). In support of a general need to incorporate *in vivo* results into interpretations based on
608 structural information, recent data from Nilaweera et al. demonstrate the importance of studying the
609 TonB system and its outer membrane TBDTs in their native cellular environment compared to *in vitro*
610 studies (93).

611 Evidence for the *in vivo* existence of ExbB tetramers and MotA tetramers (as opposed to
612 pentamers) is equally persuasive, and has the advantage that all required proteins, known and unknown,
613 are present in whole cells (79-81). For example, ExbB formaldehyde cross-links as a dimer of
614 homodimers *in vivo* (80). In another example, ExbD photo-cross-links to TonB *in vivo* through residues
615 that boundary its transmembrane domain suggesting that the ExbD and TonB transmembrane domains
616 are at some point adjacent (63), a result seemingly at odds with the structural data where the lumen of an
617 ExbB pentamer cannot accommodate additional transmembrane domains beyond the two of ExbD.
618 Heterodimerization of TonB-ExbD transmembrane domains would be consistent with Stage II in the
619 proposed energy transduction cycle (Fig. 2).

620 While *in vivo* studies of the TonB system have admittedly not always been interpreted correctly
621 [see (39) subsequently corrected in (94)], it is also worth noting that structural studies have failed to
622 correctly represent *in vivo* conformations of TonB carboxy terminal homodimers (41) and important
623 interactions between the TonB carboxy terminus and TBDTs FhuA and BtuB proteins (40). Structural

624 studies have also missed interactions between the TonB carboxy terminal amphipathic helix and TBDT
625 FepA (18). Additionally, Cys substitutions that formed ExbD disulfide-linked homodimers cannot be
626 modeled on the ExbD NMR structure without significant distortion (36). It seems possible that elements
627 of the model based on *in vivo* data summarized in Fig. 2 could provide important insights that have not
628 otherwise been gained by structural analysis. Also, considering the parable of the blind men and the
629 elephant, could there be *in vivo* equilibria among the several proposed ratios of TonB:ExbB:ExbD (11,
630 25, 80, 95, 96)?
631 Given the complexity and dynamic nature of the differing protein-protein interactions that occur
632 in each system, a true understanding of their mechanisms awaits *in vivo* data and *in vitro* structural
633 models that are significantly more congruent. Currently, much of the *in vivo* data for all three PMF-
634 dependent systems remains to be rationally incorporated into models arising from structural analyses.
635
636 *ExbD L132 is a non-essential residue*. Braun et al. isolated a spontaneous ExbD L132Q mutant
637 that was inactive, the first to demonstrate the importance of ExbD in all TonB system activities (43). In
638 this work, the construction and expression of all possible amino acid substitutions at *exbD* codon 132
639 showed that L132 is not a mechanistically important residue, even though L132Q prevents
640 formaldehyde crosslinking to TonB and stalls the energy transduction cycle at Stage I [Fig. 2; (42)].
641 Because other structurally diverse substitutions such as L132C and L132W were fully active, the L132Q
642 mutation likely caused structural distortion that prevented productive ExbD-TonB interaction.
643
644 *ExbD as a target for a novel antibiotic*. The TonB system has been recognized as a potential
645 target for novel antibiotics for many years because bacteria need sufficient iron to mount infection in
646 their hosts, which have evolved to sequester it from them (97-103). There appears to be an escalating
647 battle between bacterial pathogen and host, starting with the deliberately low levels of iron in body

648 fluids that can be thwarted by the specialized high-affinity iron acquisition systems such as the TonB
649 system that bacteria use to retrieve it (9).

650 TonB protein undergoes three different protein-protein interactions during an energy
651 transduction cycle: TonB-TonB, TonB-ExbD, and TonB-TBDT (Fig. 2). Clues that these could
652 constitute targets for intervention arise because overexpression of TonB exhibits a dominant negative
653 gene dosage effect. Proteolytic fragments of TonB that are produced when the level of TonB exceeds
654 the level of ExbB needed to proteolytically stabilize it can competitively inhibit energy transduction
655 (104, 105). An exogenously added peptide derived from a conserved consensus sequence known as the
656 "TonB box" in TBDTs showed promise (106) but was not examined further.

657 Shotgun and rational design approaches have also been used to search for compounds that could
658 inhibit the TonB system. High-throughput screening of small molecule libraries have identified
659 compounds that inhibit TonB system activity (107, 108). However, none of the compounds was shown
660 to directly target the TonB system and potential modes of inhibition were not identified.

661 Compounds that inhibit individual TonB-TBDT interactions might not be therapeutically optimal
662 since TonB interacts differently with the several different TBDTs of *E. coli* K12, which could
663 potentially diminish or eliminate the inhibition (41, 109). The essential TonB-ExbD interaction
664 appeared to be a better target since each protein and their interaction are required for energy transduction
665 through all TBDTs (Fig. 2).

666 We were expecting to discover that a peptide that is inhibitory when supplied endogenously
667 [residues 44-63; (63)] would also be inhibitory if supplied exogenously as a cyclic peptide (residues 45-
668 51), but that was not the case. Possibly it had no effect because it was too short or possibly because an
669 insufficient amount was able to cross the outer membrane and reach the periplasm. Instead, the cyclic
670 peptide cyc-IFFRA, derived from ExbD periplasmic domain residues 102-106 in a region that interacted
671 with the periplasmic domain of TonB prevented the formation of the essential ExbD-TonB complex *in*
672 *vivo* and inhibited TonB system activity. Because the peptide was cyclic and lacked an OmpT

673 recognition site, it appeared to have largely survived proteolysis by envelope proteases. It would be
674 interesting to survey the effect of this peptide on ESKAPE or other Gram-negative pathogens. The use
675 of customized cyclic peptides to inhibit the essential ExbD-TonB interaction in Gram-negative bacteria
676 could serve as a prototype for future antibiotic development.
677

678 **MATERIALS AND METHODS**

679

680 *Strains and plasmids*. Plasmids used in this work are listed in Table 5. Transmembrane domain codons
681 23-43 of *exbD* were engineered individually to Cys codons by site-directed mutagenesis PCR on
682 plasmid pKP999 which encodes wild type ExbD expressed from a propionate-inducible promoter (29).
683 Open reading frames of all *exbD* mutants were sequenced at the Penn State Genomics Core Facility,
684 University Park, PA to rule out unintended base changes. The various individual Cys- substituted
685 mutants were transformed to strains RA1045 [(*ΔexbD, ΔtolQR*); (54)], RA1017 [(*ΔexbBD, ΔtolQRA*);
686 (110)], and KP1509 [(*ΔexbD, ΔtolQR, ΔtonB*); (29)] as described in the figure legends. All three strains
687 are derivatives of W3110 (111). For studies of ExbD cyclic peptides, strain SH03 (W3110, *tolC*::Tn*10*)
688 and KP1477 [W3110, Δ*tonB* (112)] were used.

689

690 *Media and culture conditions*. Luria-Bertani (LB), tryptone (T), and M9 minimal salts media were
691 prepared as described previously (113, 114). Except for plasmid-less strains, all liquid cultures, agar
692 plates, and T-top agar were supplemented with 35 $\mu$g of chloramphenicol/ml and plasmid-specific levels
693 of propionate were added during the assay for the expression of ExbD cysteine substituted proteins at
694 chromosomal levels as determined by immunoblot. M9 salts were supplemented with 1.0% glycerol
695 (wt/vol), 0.4 mg of thiamine/ml, 1 mM $MgSO_4$, 0.5 mM $CaCl_2$, 0.2% Casamino Acids (wt/vol), 40 mg
696 of tryptophan/ml, and 1.85 $\mu$M $FeCl_3$. Cultures were grown at 37°C with continuous aeration.

697

698 *Sensitivity to colicins and bacteriophage*. To measure the relative activity of ExbD mutants, strains
699 expressing ExbD mutants at chromosomal levels were grown to mid-logarithmic phase in T-broth and
700 plated in T-top agar on T-agar plates containing 35 $\mu$g of chloramphenicol/ml. The appropriate
701 concentration of propionate inducer required for chromosomal level expression of each mutant was
702 determined by immunoblotting and was present in growth media throughout the assay. 5-fold and 10-

703 fold dilutions of colicin or bacteriophage, respectively, were spotted on the inoculated T-top layer. The
704 zones of clearing were recorded after 18 h incubation at 37°C (56, 115).
705
706 *Iodine mediated and spontaneous disulfide cross-linking*. Cells grown overnight in LB were subcultured
707 1:100 into T-broth with various amounts of Na-propionate to achieve chromosomal levels of expression
708 (from 0.0-1.0 mM and in the case of ExbD V29C, glucose at 0.005% was added to repress expression).
709 At mid-exponential phase, 0.8 $A_{550}$-ml of cells were pelleted, washed and suspended in 100 $\mu$l of cross-
710 linking buffer (20mM sodium phosphate, pH 7.4, 150mM NaCl). Then cells were treated with 0.2 mM
711 iodine ($I_2$) from a 20 mM stock solution in ethanol and kept on ice for 10 min. Unreacted free Cys
712 residues were blocked with 20 mM *N*-ethylmaleimide (NEM) for 5 min on ice (46). Cells were then
713 precipitated on ice with equal volume of 20% TCA. Pellets were suspended in SDS gel sample buffer
714 supplemented with 50mM iodoacetamide and without β-mercaptoethanol (β-ME) (116). To check the
715 level of protein expression, 0.2 $A_{550}$-ml of mid-exponential phase cells from the experimental samples
716 were harvested immediately on ice with equal volumes of 20% TCA and solubilized in SDS gel sample
717 buffer containing β-ME. A kinetic study of dimer formation showed completion of iodine-mediated
718 disulfide cross-linking within 15 sec of incubation on ice (data not shown). Both iodine-treated non-
719 reduced and β-ME-treated reduced samples were resolved on 15% SDS-polyacrylamide gels and
720 immunoblotted with ExbD-specific polyclonal antibody (11). Equal loads were confirmed by Coomassie
721 staining of the PVDF membrane used for the immunoblot. For spontaneous disulfide cross-linking,
722 iodine and NEM were omitted.
723
724 In vivo *photo-cross-linking*. Plasmid pEVOL encodes an orthogonal tRNA synthetase and a
725 corresponding orthogonal tRNACUA that recognizes amber (UAG) codons (117). Plasmids with amber
726 substitutions in *exbD* were engineered, co-expressed with pEVOL in RA1045 (W3110, Δ*exbD*, Δ*tolQR*)
727 and processed as previously described (17). At $A_{550}$ of ~0.2, sub-cultures in supplemented M9 minimal

728 media were treated with 0.004% arabinose to induce expression of the tRNA synthetase/tRNA pair from
729 pEVOL, 0.8 mM of the photo-cross-linkable amino acid p-Benzoyl-L-phenylalanine (pBpa; Bachem
730 AG, www.bachem.com) and levels of propionate required for ExbD protein expression at near-
731 chromosomal levels. 2.0 $A_{550}$-ml aliquots were harvested at $A_{550} \sim 0.5$, pelleted at room temperature and
732 suspended in 2.0 ml supplemented M9 media (as described above with 1.85 μM $FeCl_3$ instead of 37 μM,
733 and without antibiotics, pBpa, and propionate). Equal volumes of each sample were transferred into
734 single wells of each of two 24-well plates (NEST Cell Culture Plate, cat: 702001). One plate was
735 irradiated with 365-nm light for 30 min on ice and the second plate was simultaneously incubated in the
736 dark for 30 min on ice. Samples were precipitated with an equal volume of 20% TCA as described
737 previously and processed for immunoblot analysis with ExbD-specific polyclonal antibodies and TonB-
738 specific monoclonal antibodies (11, 118). Equal loads were confirmed by Coomassie staining of the
739 PVDF membrane used for the immunoblot.
740
741 *Initial rates of [$^{55}$Fe]-ferrichrome transport*. The initial rates of iron transport were determined as
742 described previously (56, 115). Mid-exponential-phase subcultures were pelleted and suspended in iron
743 transport assay media, and the initial rates of [$^{55}$Fe]-ferrichrome transport were determined. Equal
744 proportions of the suspended cells were precipitated with an equal volume of 20% TCA to confirm the
745 chromosomal level expression of ExbD mutants by immunoblot. Precipitates were solubilized in SDS
746 gel sample buffer (116), electrophoresed on a 15% SDS polyacrylamide gel and immunobotted with
747 anti-ExbD polyclonal antibody (11). Inhibitory ExbD-based cyclic peptides were purchased from
748 GenScript USA, Inc., Piscataway, New Jersey. Assay of equal numbers of cells in each sample was
749 confirmed by Coomassie staining of the PVDF membrane used for the immunoblots.
750
751
752 *In-vivo formaldehyde cross-linking*

753 Cultures were grown overnight to saturation in LB broth at 37°C with aeration. The saturated cultures
754 were subsequently subcultured 1:100 in supplemented M9 minimal media. At mid-exponential phase,
755 volumes were adjusted to harvest 0.5 $A_{550}$-ml of cells. Bacteria were suspended in sodium phosphate
756 buffer (pH 6.8) and treated for 15 min at room temperature with 1% monomeric formaldehyde (Electron
757 Microscopy Sciences Cat #15710) as previously described (29). Following formaldehyde treatment,
758 bacteria were pelleted and suspended in SDS gel sample buffer (116), with equal cell numbers loaded on
759 SDS 13% polyacrylamide gels. ExbD complexes and TonB complexes were detected by
760 immunoblotting with ExbD-specific polyclonal antibodies and TonB-specific monoclonal antibodies,
761 respectively (11, 118). Equal loads were confirmed by Coomassie staining of the PVDF membrane used
762 for the immunoblot.
763
764
765 **Acknowledgements**
766 We thank Ann Ollis and Christine Dubowy for construction and assay of the Cys relocation mutants. We
767 thank Yan Shipelskiy for construction and assay of ExbD D25X mutants. We thank Garrick Treaster,
768 Anne Ollis, and Elise Zhao for construction and characterization of mutations at ExbD residue L132.
769 We thank Erica Johnson for construction of several amber mutations in *exbD*. We thank William Russ
770 and Donald Engelman for TOXCAT vectors and *E. coli* NT326 cells, and Kevin Bertrand and Stuart
771 Huntley for the gift of SH03. We thank Ray Larsen for editorial feedback on the manuscript. Support
772 from NIAID R21 AI113622, NIGMS R01 GM112710, and Violet S. Postle is gratefully acknowledged.

773 **REFERENCES**

774


775 1. **Cornelissen CN, Hollander A.** 2011. TonB-Dependent transporters expressed by *Neisseria*
776 *gonorrhoeae*. Front Microbiol **2:**117.

777 2. **Noinaj N, Buchanan SK, Cornelissen CN.** 2012. The transferrin-iron import system from
778 pathogenic *Neisseria* species. Mol Microbiol **86:**246-257.

779 3. **Krewulak KD, Vogel HJ.** 2011. TonB or not TonB: is that the question? Biochemistry and cell
780 biology **89:**87-97.

781 4. **Kuehl CJ, Crosa JH.** 2010. The TonB energy transduction systems in *Vibrio* species. Future
782 Microbiology **5:**1403-1412.

783 5. **Blanvillain S, Meyer D, Boulanger A, Lautier M, Guynet C, Denance N, Vasse J, Lauber E,**
784 **Arlat M.** 2007. Plant carbohydrate scavenging through TonB-Dependent receptors: A feature
785 shared by phytopathogenic and aquatic bacteria. PLoS ONE **2:**e224.

786 6. **Cescau S, Cwerman H, Letoffe S, Delepelaire P, Wandersman C, Biville F.** 2007. Heme
787 acquisition by hemophores. Biometals **20:**603-613.

788 7. **Lohmiller S, Hantke K, Patzer SI, Braun V.** 2008. TonB-dependent maltose transport by
789 *Caulobacter crescentus*. Microbiology **154:**1748-1754.

790 8. **Schauer K, Rodionov DA, de Reuse H.** 2008. New substrates for TonB-dependent transport: do
791 we only see the 'tip of the iceberg'? Trends Biochem Sci **33:**330-338.

792 9. **Sheldon JR, Laakso HA, Heinrichs DE.** 2016. Iron acquisition strategies of bacterial
793 pathogens. Microbiol Spectr **4**.

794 10. **Kadner RJ, Heller KJ.** 1995. Mutual inhibition of cobalamin and siderophore uptake systems
795 suggests their competition for TonB function. J Bacteriol **177:**4829-4835.

796 11. **Higgs PI, Larsen RA, Postle K.** 2002. Quantitation of known components of the *Escherichia*
797 *coli* TonB-dependent energy transduction system: TonB, ExbB, ExbD, and FepA. Mol Microbiol
798 **44:**271-281.
799 12. **Gresock MG, Kastead KA, Postle K.** 2015. From homodimer to heterodimer and back:
800 Elucidating the TonB energy transduction cycle. J Bacteriol **197:**3433-3445.
801 13. **Larsen RA, Thomas MG, Postle K.** 1999. Protonmotive force, ExbB and ligand-bound FepA
802 drive conformational changes in TonB. Mol Microbiol **31:**1809-1824.
803 14. **Higgs PI, Letain TE, Merriam KK, Burke NS, Park H, Kang C, Postle K.** 2002. TonB
804 interacts with nonreceptor proteins in the outer membrane of *Escherichia coli*. J Bacteriol
805 **184:**1640-1648.
806 15. **Cadieux N, Kadner RJ.** 1999. Site-directed disulfide bonding reveals an interaction site
807 between energy-coupling protein TonB and BtuB, the outer membrane cobalamin transporter.
808 Proc Natl Acad Sc U. S. A. **96:**10673-10678.
809 16. **Ogierman M, Braun V.** 2003. Interactions between the outer membrane ferric citrate
810 transporter FecA and TonB: studies of the FecA TonB box. J Bacteriol **185:**1870-1885.
811 17. **Gresock MG, Postle K.** 2017. Going outside the TonB Box: Identification of novel FepA-TonB
812 interactions *in vivo*. J Bacteriol **199:**e00649-00616.
813 18. **Postle K, Kho K, Gresock MG, Ghosh J, Larsen RA.** 2021. Identification of new *in vivo*
814 TonB-FepA rendevous sites. bioRxiv. doi: https://doi.org/10.1101/2021.12.08.471779
815 19. **Plastow GS, Holland IB.** 1979. Identification of an *Escherichia coli* inner membrane
816 polypeptide specified by a lambda-*tonB* transducing phage. Biochem. Biophys Res Commun
817 **90:**1007-1014.
818 20. **Kampfenkel K, Braun V.** 1992. Membrane topology of the *Escherichia coli* ExbD protein. J
819 Bacteriol **174:**5485-5487.

820 21. **Roof SK, Allard JD, Bertrand KP, Postle K.** 1991. Analysis of *Escherichia coli* TonB
821 membrane topology by use of PhoA fusions. J Bacteriol **173:**5554-5557.
822 22. **Kampfenkel K, Braun V.** 1993. Topology of the ExbB protein in the cytoplasmic membrane of
823 *Escherichia coli*. J Biol Chem **268:**6050-6057.
824 23. **Fischer E, Günter K, Braun V.** 1989. Involvement of ExbB and TonB in transport across the
825 outer membrane of *Escherichia coli*: phenotypic complementation of *exb* mutants by
826 overexpressed *tonB* and physical stabilization of TonB by ExbB. J Bacteriol **171:**5127-5134.
827 24. **Karlsson M, Hannavy K, Higgins CF.** 1993. ExbB acts as a chaperone-like protein to stabilize
828 TonB in the cytoplasm. Mol Microbiol **8:**389-396.
829 25. **Pramanik A, Zhang F, Schwarz H, Schreiber F, Braun V.** 2010. ExbB protein in the
830 cytoplasmic membrane of *Escherichia coli* forms a stable oligomer. Biochemistry **49:**8721-8728.
831 26. **Swayne C, Postle K.** 2011. Taking the *Escherichia coli* TonB transmembrane domain
832 "Offline"? Non-protonatable Asn substitutes fully for TonB His20. J Bacteriol **193:**3693-3701.
833 27. **Baker KR, Postle K.** 2013. Mutations in *Escherichia coli* ExbB transmembrane domains
834 identify scaffolding and signal transduction functions and exclude participation in a proton
835 pathway. J Bacteriol **195:**2898-2911.
836 28. **Skare JT, Ahmer BMM, Seachord CL, Darveau RP, Postle K.** 1993. Energy transduction
837 between membranes - TonB, a cytoplasmic membrane protein, can be chemically cross-linked *in*
838 *vivo* to the outer membrane receptor FepA. J Biol Chem **268:**16302-16308.
839 29. **Ollis AA, Manning M, Held KG, Postle K.** 2009. Cytoplasmic membrane protonmotive force
840 energizes periplasmic interactions between ExbD and TonB. Mol Microbiol **73:**466-481.
841 30. **Pawelek PD, Croteau N, Ng-Thow-Hing C, Khursigara CM, Moiseeva N, Allaire M,**
842 **Coulton JW.** 2006. Structure of TonB in complex with FhuA, *E. coli* outer membrane receptor.
843 Science **312:**1399-1402.

844 31. **Shultis DD, Purdy MD, Banchs CN, Wiener MC.** 2006. Outer membrane active transport:
845 structure of the BtuB:TonB complex. Science **312:**1396-1399.
846 32. **Khursigara CM, De Crescenzo G, Pawelek PD, Coulton JW.** 2004. Enhanced binding of
847 TonB to a ligand-loaded outer membrane receptor. Role of the oligomeric state of TonB in
848 formation of a functional FhuA-TonB complex. J Biol Chem **279:**7405-7412.
849 33. **Khursigara CM, De Crescenzo G, Pawelek PD, Coulton JW.** 2005. Kinetic analyses reveal
850 multiple steps in forming TonB-FhuA complexes from *Escherichia coli*. Biochemistry **44:**3441-
851 3453.
852 34. **Freed DM, Lukasik SM, Sikora A, Mokdad A, Cafiso DS.** 2013. Monomeric TonB and the
853 Ton Box are required for the formation of a high-affinity transporter-TonB complex.
854 Biochemistry **52:**2638-2648.
855 35. **Ollis AA, Kumar A, Postle K.** 2012. The ExbD periplasmic domain contains distinct functional
856 regions for two stages in TonB energization. J Bacteriol **194:**3069-3077.
857 36. **Ollis AA, Postle K.** 2011. The same periplasmic ExbD residues mediate *in vivo* interactions
858 between ExbD homodimers and ExbD-TonB heterodimers. J Bacteriol **193:**6852-6863.
859 37. **Skare JT, Roof SK, Postle K.** 1989. A mutation in the amino terminus of a hybrid TrpC-TonB
860 protein relieves overproduction lethality and results in cytoplasmic accumulation. J Bacteriol
861 **171:**4442-4447.
862 38. **Larsen RA, Wood GE, Postle K.** 1993. The conserved proline-rich motif is not essential for
863 energy transduction by *Escherichia coli* TonB protein. Mol Microbiol **10:**943-953.
864 39. **Larsen RA, Letain TE, Postle K.** 2003. *In vivo* evidence of TonB shuttling between the
865 cytoplasmic and outer membrane in *Escherichia coli*. Mol Microbiol **49:**211-218.
866 40. **Vakharia-Rao H, Kastead KA, Savenkova MI, Bulathsinghala CM, Postle K.** 2007. Deletion
867 and substitution analysis of the *Escherichia coli* TonB Q160 region. J Bacteriol **189:**4662-4670.

868 41. **Postle K, Kastead KA, Gresock MG, Ghosh J, Swayne CD.** 2010. The TonB dimeric crystal
869 structures do not exist *in vivo*. mBio **1:**e00307-00310.
870 42. **Ollis AA, Postle K.** 2012. ExbD mutants define initial stages in TonB energization. J Mol Biol
871 **415:**237-247.
872 43. **Braun V, Gaisser S, Herrmann C, Kampfenkel K, Killman H, Traub I.** 1996. Energy-
873 coupled transport across the outer membrane of *Escherichia coli*: ExbB binds ExbD and TonB
874 *in vitro*, and leucine 132 in the periplasmic region and aspartate 25 in the transmembrane region
875 are important for ExbD activity. J Bacteriol **178:**2836-2845.
876 44. **Ollis AA, Postle K.** 2012. Identification of functionally important TonB-ExbD periplasmic
877 domain interactions *in vivo*. J Bacteriol **194:**3078-3087.
878 45. **Eick-Helmerich K, Braun V.** 1989. Import of biopolymers into *Escherichia coli*: nucleotide
879 sequences of the *exbB* and *exbD* genes are homologous to those of the *tolQ* and *tolR* genes,
880 respectively. J Bacteriol **171:**5117-5126.
881 46. **Braun TF, Blair DF.** 2001. Targeted disulfide cross-linking of the MotB protein of *Escherichia*
882 *coli*: evidence for two H(+) channels in the stator complex. Biochemistry **40:**13051-13059.
883 47. **Zhang XY, Goemaere EL, Thome R, Gavioli M, Cascales E, Lloubes R.** 2009. Mapping the
884 Interactions between *Escherichia coli* Tol Subunits: Rotation of the TolR Transmembrane Helix.
885 J Biol Chem **284:**4275-4282.
886 48. **Cascales E, Lloubes R, Sturgis JN.** 2001. The TolQ-TolR proteins energize TolA and share
887 homologies with the flagellar motor proteins MotA-MotB. Mol Microbiol **42:**795-807.
888 49. **Zhou J, Sharp LL, Tang HL, Lloyd SA, Billings S, Braun TF, Blair DF.** 1998. Function of
889 protonatable residues in the flagellar motor of *Escherichia coli*: a critical role for Asp 32 of
890 MotB. J Bacteriol **180:**2729-2735.
891 50. **Celia H, Noinaj N, Buchanan SK.** 2020. Structure and stoichiometry of the Ton molecular
892 motor. Int J Mol Sci **21**.

893 51. **Deme JC, Johnson S, Vickery O, Aron A, Monkhouse H, Griffiths T, James RH, Berks BC,**
894 **Coulton JW, Stansfeld PJ, Lea SM.** 2020. Structures of the stator complex that drives rotation
895 of the bacterial flagellum. Nat Microbiol **5:**1553-1564.
896 52. **Santiveri M, Roa-Eguiara A, Kuhne C, Wadhwa N, Hu H, Berg HC, Erhardt M, Taylor**
897 **NMI.** 2020. Structure and function of stator units of the bacterial flagellar motor. Cell **183:**244-
898 257 e216.
899 53. **Braun V.** 1989. The structurally related *exbB* and *tolQ* genes are interchangeable in conferring
900 *tonB*-dependent colicin, bacteriophage, and albomycin sensitivity. J Bacteriol **171:**6387-6390.
901 54. **Brinkman KK, Larsen RA.** 2008. Interactions of the energy transducer TonB with noncognate
902 energy-harvesting complexes. J Bacteriol **190:**421-427.
903 55. **Lloubes R, Goemaere E, Zhang X, Cascales E, Duche D.** 2012. Energetics of colicin import
904 revealed by genetic cross-complementation between the Tol and Ton systems. Biochem Soc
905 Trans **40:**1480-1485.
906 56. **Larsen RA, Chen GJ, Postle K.** 2003. Performance of standard phenotypic assays for TonB
907 activity, as evaluated by varying the level of functional, wild-type TonB. J Bacteriol **185:**4699-
908 4706.
909 57. **Bernsel A, Viklund H, Hennerdal A, Elofsson A.** 2009. TOPCONS: consensus prediction of
910 membrane protein topology. Nuc Acids Res **37:**W465-468.
911 58. **Russ WP, Engelman DM.** 1999. TOXCAT: a measure of transmembrane helix association in a
912 biological membrane. Proc Natl Acad Sci U S A **96:**863-868.
913 59. **Kopp DR, Postle K.** 2020. The intrinsically disordered region of ExbD is required for signal
914 transduction. J Bacteriol **202:**e00687-00619.
915 60. **Garcia-Herrero A, Peacock RS, Howard SP, Vogel HJ.** 2007. The solution structure of the
916 periplasmic domain of the TonB system ExbD protein reveals an unexpected structural
917 homology with siderophore-binding proteins. Mol Microbiol **66:**872-889.

918 61. **Treptow NA, Shuman HA.** 1985. Genetic evidence for substrate and periplasmic-binding-
919 protein recognition by the MalF and MalG proteins, cytoplasmic membrane components of the
920 *Escherichia coli* maltose transport system. J Bacteriol **163:**654-660.
921 62. **Postle K, Larsen R.** 2004. The TonB, ExbB, and ExbD Proteins, p. 96-112. *In* Crosa JH, Mey
922 AR, Payne SM (ed.), Iron transport in Bacteria. ASM Press, Washington D.C.
923 63. **Kopp DR, Postle K.** 2020. An ExbD disordered domain peptide inhibits TonB system activity.
924 bioRxiv doi: https://doi.org/10.1101/2020.01.05.895219.
925 64. **Silver LL.** 2011. Challenges of antibacterial discovery. Clin Microbiol Rev **24:**71-109.
926 65. **Dyson HJ, Wright PE.** 2005. Intrinsically unstructured proteins and their functions. Nat Rev
927 Mol Cell Biol **6:**197-208.
928 66. **McCarter JD, Stephens D, Shoemaker K, Rosenberg S, Kirsch JF, Georgiou G.** 2004.
929 Substrate specificity of the *Escherichia coli* outer membrane protease OmpT. J Bacteriol
930 **186:**5919-5925.
931 67. **Chakravorty S, Shipelskiy Y, Kumar A, Majumdar A, Yang T, Nairn BL, Newton SM,**
932 **Klebba PE.** 2019. Universal fluorescent sensors of high-affinity iron transport, applied to
933 ESKAPE pathogens. J Biol Chem **294:**4682-4692.
934 68. **Young L, Jernigan RL, Covell DG.** 1994. A role for surface hydrophobicity in protein-protein
935 recognition. Protein Sci **3:**717-729.
936 69. **Bogan AA, Thorn KS.** 1998. Anatomy of hot spots in protein interfaces. J Mol Biol **280:**1-9.
937 70. **Nikaido H.** 2003. Molecular basis of bacterial outer membrane permeability revisited. Microbiol
938 Mol Biol Rev **67:**593-656.
939 71. **Hinchliffe P, Symmons MF, Hughes C, Koronakis V.** 2013. Structure and operation of
940 bacterial tripartite pumps. Annu Rev Microbiol **67:**221-242.
941 72. **Ghosh J, Postle K.** 2005. Disulphide trapping of an *in vivo* energy-dependent conformation of
942 *Escherichia coli* TonB protein. Mol Microbiol **55:**276-288.

943 73. **Toews J, Rogalski JC, Clark TJ, Kast J.** 2008. Mass spectrometric identification of
944 formaldehyde-induced peptide modifications under in vivo protein cross-linking conditions. Anal
945 Chim Acta **618:**168-183.
946 74. **Means GE, Feeney RE.** 1971. Chemical modification of proteins. Holden-Day, Inc., San
947 Francisco, Calif.
948 75. **Klebba PE, Newton SMC, Six DA, Kumar A, Yang T, Nairn BL, Munger C, Chakravorty**
949 **S.** 2021. Iron acquisition systems of Gram-negative bacterial pathogens define TonB-dependent
950 pathways to novel antibiotics. Chem Rev **121:**5193-5239.
951 76. **Braun V.** 2006. Energy transfer between biological membranes. ACS Chem Biol **1:**352-354.
952 77. **Gerding MA, Ogata Y, Pecora ND, Niki H, de Boer PA.** 2007. The trans-envelope Tol-Pal
953 complex is part of the cell division machinery and required for proper outer-membrane
954 invagination during cell constriction in *E. coli.* Mol Microbiol **63:**1008-1025.
955 78. **Kojima S, Blair DF.** 2001. Conformational change in the stator of the bacterial flagellar motor.
956 Biochemistry **40:**13041-13050.
957 79. **Bulathsinghala CM, Jana B, Baker KR, Postle K.** 2013. ExbB cytoplasmic loop deletions
958 cause immediate, proton motive force-independent growth arrest. J Bacteriol **195:**4580-4591.
959 80. **Jana B, Manning M, Postle K.** 2011. Mutations in the ExbB cytoplasmic carboxy terminus
960 prevent energy-dependent interaction between the TonB and ExbD periplasmic domains. J
961 Bacteriol **193:**5649-5657.
962 81. **Braun TF, Al-Mawsawi LQ, Kojima S, Blair DF.** 2004. Arrangement of core membrane
963 segments in the MotA/MotB proton-channel complex of *Escherichia coli*. Biochemistry **43:**35-
964 45.
965 82. **Koebnik R.** 1995. Proposal for a peptidoglycan-associating alpha-helical motif in the C-terminal
966 regions of some bacterial cell-surface proteins. Mol Microbiol **16:**1269-1270.

967 83. **Roujeinikova A.** 2008. Crystal structure of the cell wall anchor domain of MotB, a stator
968 component of the bacterial flagellar motor: implications for peptidoglycan recognition. Proc Natl
969 Acad Sci U S A **105:**10348-10353.
970 84. **Hosking ER, Vogt C, Bakker EP, Manson MD.** 2006. The *Escherichia coli* MotAB proton
971 channel unplugged. J Mol Biol **364:**921-937.
972 85. **Braun V, Herrmann C.** 1993. Evolutionary relationship of uptake systems for biopolymers in
973 *Escherichia coli*: cross-complementation between the TonB-ExbB-ExbD and the TolA-TolQ-
974 TolR proteins. Mol Microbiol **8:**261-268.
975 86. **Goemaere EL, Devert A, Lloubes R, Cascales E.** 2007. Movements of the TolR C-terminal
976 domain depend on TolQR ionizable key residues and regulate activity of the Tol complex. J Biol
977 Chem **282:**17749-17757.
978 87. **Szczepaniak J, Press C, Kleanthous C.** 2020. The multifarious roles of Tol-Pal in Gram-
979 negative bacteria. FEMS Microbiol Rev **44:**490-506.
980 88. **Wojdyla JA, Cutts E, Kaminska R, Papadakos G, Hopper JTS, Stansfeld PJ, Staunton D,**
981 **Robinson CV, Kleanthous C.** 2015. Structure and function of the *Escherichia coli* Tol-Pal
982 stator protein TolR. J Biol Chem **290:**26675-26687.
983 89. **Celia H, Botos I, Ni X, Fox T, De Val N, Lloubes R, Jiang J, Buchanan SK.** 2019. Cryo-EM
984 structure of the bacterial Ton motor subcomplex ExbB-ExbD provides information on structure
985 and stoichiometry. Commun Biol **2:**358.
986 90. **Hennell James R, Deme JC, Kjr A, Alcock F, Silale A, Lauber F, Johnson S, Berks BC, Lea**
987 **SM.** 2021. Structure and mechanism of the proton-driven motor that powers type 9 secretion and
988 gliding motility. Nat Microbiol **6:**221-233.
989 91. **Ratliff AC, Buchanan SK, Celia H.** 2021. Ton motor complexes. Curr Opin Struct Biol **67:**95-
990 100.

991 92. **Guihard G, Boulanger P, Benedetti H, Lloubes R, Besnard M, Letellier L.** 1994. Colicin A
992 and the Tol proteins involved in its translocation are preferentially located in the contact sites
993 between the inner and outer membranes of *Escherichia coli* cells. J Biol Chem **269:**5874-5880.
994 93. **Nilaweera TD, Nyenhuis DA, Cafiso DS.** 2021. Structural intermediates observed only in intact
995 *Escherichia coli* indicate a mechanism for TonB-dependent transport. Elife **10:**e68548.
996 94. **Gresock MG, Savenkova MI, Larsen RA, Ollis AA, Postle K.** 2011. Death of the TonB
997 shuttle hypothesis. Front Microbiol **2:**206.
998 95. **Pramanik A, Hauf W, Hoffmann J, Cernescu M, Brutschy B, Braun V.** 2011. Oligomeric
999 structure of ExbB and ExbB-ExbD isolated from *Escherichia coli* as revealed by LILBID-mass
1000 spectrometry. Biochemistry **50:8950-6**
1001 96. **Sverzhinsky A, Chung JW, Deme JC, Fabre L, Levey KT, Plesa M, Carter DM,**
1002
1003 **Lypaczewski P, Coulton JW.** 2015. Membrane protein complex ExbB4-ExbD1-TonB1 from
1004
1005 *Escherichia coli* demonstrates conformational plasticity. J Bacteriol **197**:1873-85.
1006
1007 97. **Bullen JJ, Ward CG.** 1988. Iron and infection. Br Med J **296:**1539.
1008 98. **Bullen JJ.** 1981. The significance of iron in infection. Rev Infect Dis **3:**1127-1138.
1009 99. **Bullen JJ, Rogers HJ, Griffiths E.** 1978. Role of iron in bacterial infection. Curr Top Microbiol
1010 Immunol **80:**1-35.
1011 100. **Parrow NL, Fleming RE, Minnick MF.** 2013. Sequestration and scavenging of iron in
1012 infection. Infection and immunity **81:**3503-3514.
1013 101. **Drakesmith H, Prentice AM.** 2012. Hepcidin and the iron-infection axis. Science **338:**768-772.
1014 102. **Bullen JJ, Griffiths E.** 1999. Iron and Infection, 2nd ed. John Wiley & Sons, Chichester, West
1015 Sussex.
1016 103. **Sparling PF.** 1998. Iron and infection. Clin Infect Dis **27:**1367-1368.
1017 104. **Mann BJ, Holroyd CD, Bradbeer C, Kadner RJ.** 1986. Reduced activity of TonB-dependent
1018 functions in strains of *Escherichia coli*. *FEMS Lett.* **33:**255-260.

1019 105. **Howard SP, Herrmann C, Stratilo CW, Braun V.** 2001. *In vivo* synthesis of the periplasmic
1020 domain of TonB inhibits transport through the FecA and FhuA iron siderophore transporters of
1021 *Escherichia coli*. J Bacteriol **183:**5885-5895.
1022 106. **Tuckman M, Osburne MS.** 1992. *In vivo* inhibition of TonB-dependent processes by a TonB
1023 box consensus pentapeptide. J Bacteriol **174:**320-323.
1024 107. **Nairn BL, Eliasson OS, Hyder DR, Long NJ, Majumdar A, Chakravorty S, McDonald P,**
1025 **Roy A, Newton SM, Klebba PE.** 2017. Fluorescence high-throughput screening for inhibitors
1026 of TonB action. J Bacteriol **199**(10):e00889-16
1027 108. **Yep A, McQuade T, Kirchhoff P, Larsen M, Mobley HL.** 2014. Inhibitors of TonB function
1028 identified by a high-throughput screen for inhibitors of iron acquisition in uropathogenic
1029 *Escherichia coli* CFT073. mBio **5:**e01089-01013.
1030 109. **Ghosh J, Postle K.** 2004. Evidence for dynamic clustering of carboxy-terminal aromatic amino
1031 acids in TonB-dependent energy transduction. Mol Microbiol **51:**203-213.
1032 110. **Larsen RA, Deckert GE, Kastead KA, Devanathan S, Keller KL, Postle K.** 2007. His20
1033 provides the sole functionally significant side chain in the essential TonB transmembrane
1034 domain. J Bacteriol **189:**2825-2833.
1035 111. **Hill CW, Harnish BW.** 1981. Inversions between ribosomal RNA genes of *Escherichia coli*.
1036 Proc Natl Acad Sci.USA **78:**7069-7072.
1037 112. **Devanathan S, Postle K.** 2007. Studies on colicin B translocation: FepA is gated by TonB. Mol
1038 Microbiol **65:**441-453.
1039 113. **Shedlovsky A, Brenner S.** 1963. A chemical basis for the host-induced modification of T-even
1040 bacteriophages. Proc Natl Acad Sci U S A **50:**300-305.
1041 114. **Miller JH.** 1972. Experiments in molecular genetics. Cold Spring Harbor Laboratory Press, Cold
1042 Spring Harbor, N. Y.
1043 115. **Postle K.** 2007. TonB system, *in vivo* assays and characterization. Meth Enzymol **422:**245-269.

1044 116. **Laemmli UK.** 1970. Cleavage of structural proteins during the assembly of the head of
1045 bacteriophage T4. Nature **227:**680-685.
1046 117. **Young TS, Ahmad I, Yin JA, Schultz PG.** 2010. An enhanced system for unnatural amino acid
1047 mutagenesis in *E. coli.* J Mol Biol **395:**361-374.
1048 118. **Larsen RA, Myers PS, Skare JT, Seachord CL, Darveau RP, Postle K.** 1996. Identification
1049 of TonB homologs in the family *Enterobacteriaceae* and evidence for conservation of TonB-
1050 dependent energy transduction complexes. J Bacteriol **178:**1363-1373.
1051 119. **Ahmer BMM, Thomas MG, Larsen RA, Postle K.** 1995. Characterization of the *exbBD*
1052 operon of *Escherichia coli* and the role of ExbB and ExbD in TonB function and stability. J
1053 Bacteriol **177:**4742-4747.
1054 120. **Buchanan SK, Smith BS, Venkatramani L, Xia D, Esser L, Palnitkar M, Chakraborty R,**
1055 **van der Helm D, Deisenhofer J.** 1999. Crystal structure of the outer membrane active
1056 transporter FepA from *Escherichia coli*. Nat. Struct. Biol. **6:**56-63.
1057 121. **Yakushi T, Kojima M, Homma M.** 2004. Isolation of Vibrio alginolyticus sodium-driven
1058 flagellar motor complex composed of PomA and PomB solubilized by sucrose monocaprate.
1059 Microbiology **150:**911-920.
1060 122. **Higgs PI, Myers PS, Postle K.** 1998. Interactions in the TonB-dependent energy transduction
1061 complex: ExbB and ExbD form homomultimers. J Bacteriol **180:**6031-6038.

## TABLES

**Table 1. Phenotypes of strains producing Cys-substituted ExbD proteins**

| ExbD | ø80 | colicin B | colicin Ia | colicin M |
|---|---|---|---|---|
| W3110 | 8, 9, 8 | 6, 6, 6 | 5, 5, 5 | 4, 4, 4 |
| pExbD | 8, 8, 8 | 5, 5, 5 | 5, 5, 5 | 4, 4, 4 |
| F23C | 6, 7, 6 | 4, 4, 5 | 5, 5, 4 | 4, 4, 4 |
| I24C | 6, 5, 6 | 4, 4, 4 | 5, 5, 5 | 3, 3, 3 |
| D25C | T, T, T | T, T, T | T, T, T | T, T, T |
| V26C | 7, 7, 7 | 5, 5 ,5 | 5, 5, 5 | 4, 4, 4 |
| M27C | 7, 7, 7 | 5, 5 ,5 | 5, 5, 5 | 4, 4, 4 |
| L28C | 7, 7, 7 | 4, 4, 4 | 5, 5, 6 | 4, 4, 4 |
| V29C | 8, 7, 7 | 5, 5, 5 | 5, 5, 5 | 3, 3, 3 |
| L30C | 6, 6, 6 | 4, 5, 4 | 5, 5, 5 | 3, 3, 4 |
| L31C | 6, 6, 6 | 5, 5, 5 | 5, 5, 5 | 3, 4, 4 |
| I32C | 6, 6, 6 | 5, 6, 5 | 5, 5, 5 | 4, 4, 4 |
| I33C | 7, 7, 7 | 4, 4, 4 | 5, 5, 5 | 3, 3, 3 |
| F34C | 8, 7, 7 | 5, 5, 5 | 4, 4, 4 | 3, 3, 3 |
| M35C | 7, 7, 7 | 4, 4, 5 | 5, 5, 4 | 3, 3, 3 |
| V36C | 8, 7, 7 | 5, 5 ,5 | 4, 5, 4 | 3, 3, 3 |
| A37C | 8, 8, 8 | 5, 5, 5 | 5, 4, 5 | 4, 4, 4 |
| A38C | 7, 7, 7 | 5, 5, 5 | 4, 4, 4 | 3, 3, 4 |
| P39C | 7, 7, 7 | 4, 3 ,4 | 4, 4, 4 | 3, 3, 3 |
| L40C | 8, 8, 8 | 5, 5, 5 | 5, 5, 5 | 4, 4, 4 |
| A41C | 8, 7, 7 | 5, 5, 5 | 4, 5, 4 | 3, 3, 3 |
| T42C | 7, 7 ,7 | 5, 5, 5 | 5, 5, 5 | 3, 3, 3 |
| V43C | 8, 7, 7 | 5, 5, 5 | 5, 4, 5 | 3, 3, 3 |

Parent plasmid pExbD is pKP999. Phenotypes of ExbD mutants were evaluated in RA1045 (Δ*exbD*, Δ*tolQR*) using spot titer assays (56). Cultures with the strains expressing ExbD mutated proteins at chromosomal levels were plated on T-plates and spotted with fivefold serial dilutions of colicins and 10-fold serial dilutions of bacteriophage Φ80. Values were recorded as the reciprocal of the highest dilution at which clearing of the lawn was evident after 18 h of incubation at 37°C. 'T' indicates tolerance (insensitivity).

**Table 2. ExbD residues 23-63 form homodimers independently of ExbB**

| Plasmid | [a]34 | 62.5 | 125 | 250 | 500 | 1000 |
|---|---|---|---|---|---|---|
| [b]WT/pccKan vector | - | - | - | - | - | - |
| WT/pccGlpA | [c]n.d. | 4+ | 4+ | 4+ | 1+ | - |
| WT/pccGlpA G83I | n.d. | 2+ | +/- | - | - | - |
| WT/pccExbD$_{23-63}$ | n.d. | 4+ | 3+ | 2+ | +/- | - |
| | | | | | | |
| [d]*exbBD*/pccKan vector | - | - | - | - | - | - |
| *exbBD*/pccGlpA | 4+ | 4+ | 4+ | 3+ | 1+ | - |
| *exbBD*/pccGlpA G83I | 3+ | 2+ | 1+ | | | |
| *exbBD*/pccExbD$_{23-63}$ | 4+ | 4+ | 4+ | 3+ | 1+ | |

[a]plate concentration of chloramphenicol (µg/ml)

[b]strain NT326 is wild-type for *exbB*: [*araD*139, Δ(*argF-lac*)$_{U169}$, Δ*malE444*, *recA*1, *thi*, *strR* (61)]

[c]growth; n.d. = not determined

[d]strain NT326, made *exbB*::Tn*10* by P1vir transduction (KP1448). The Tn*10* insertion in *exbB* is polar on downstream *exbD* expression (119).

**Table 3. ExbD T42C and V43C disulfide-linked homodimers are impaired in TonB system-mediated iron transport.**

| | % rate relative to pExbD without DTT | % rate relative to pExbD with DTT |
|---|---|---|
| **RA1045** | 0.15% | |
| **W3110** | 121% | |
| **pExbD** | 100% | 100% |
| **pExbD L40C** | 101.9% | |
| **pExbD A41C** | 103.6% | |
| **pExbD T42C** | 22.9% | 77% |
| **pExbD V43C** | 9.2% | 89% |

RA1045 is [(*ΔexbD, ΔtolQR*); (54)]; W3110 is wild-type *E. coli* K12 (111); pExbD is pKP999 (29).

Percentiles of transport rates were calculated by slopes derived from linear regression analysis of the individual data points, as described in (72). See Fig. 6 B and C.

## Table 4 ExbD L132 is not an essential residue

| [a]Position 132 a.a. | [b]Active? | [c]Plasmid | [d][propionate] in mM |
|---|---|---|---|
| L | Y | pKP999 | 0.3 |
| A | - | pKP1325 | 0.3 |
| C | Y | pKP1332 | 0.5 |
| Q | - | pKP1333 | 0.5 |
| S | - | pKP1409 | 0.5 |
| V | Y | pKP1449 | 0.2 |
| D | - | pKP1455 | 0.5 |
| T | - | pKP1699 | 0.5 |
| K | - | pKP1698 | 1.0 |
| R | - | pKP1712 | 0.3 |
| H | - | pKP1701 | 0.3 |
| E | - | pKP1702 | 0.5 |
| N | - | pKP1689 | 0.5 |
| G | - | pKP1745 | 0.4 |
| P | - | pKP1703 | 0.3 |
| I | Y | pKP1697 | 0.5 |
| M | Y | pKP1696 | 0.3 |
| F | Y | pKP1713 | 0.3 |
| W | Y | pKP1700 | 0.5 |
| Y | - | pKP1744 | 0.3 |

[a]Single letter code for the amino acid substituted at ExbD residue 132.

[b]Activity of the ExbD variant as determined by iron-dependent growth in RA1045 (*ΔexbD, ΔtolQR*): Y = activity was same as wild-type *exbD* in pKP999; (-) = inactive, no growth

[c]Plasmid encoding each variant

[d]Concentration of propionate inducer used for chromosomal level of expression (mM)

**Table 5 Plasmids used in this study**

| Plasmid | Relevant phenotype | Source or reference |
|---|---|---|
| pccKan | TOXCAT system vector | (58) |
| pccGlpA | GlpA-TOXCAT fusion | (58) |
| pccGlpAG83I | GlpA G83I-TOXCAT fusion | (58) |
| pKP523 | $ExbD_{23-63}$-TOXCAT fusion | (58) |
| pKP568 | TonB(C18G) | (72) |
| pKP945 | TonB(C18G, A150C) | (29) |
| pKP999 | pPro24 expressing wild-type ExbD | (29) |
| pKP1000 | ExbD(A92C) | (29) |
| pKP1064 | ExbD(D25N) | (29) |
| pKP1394 | ExbD(F23C) | Present study |
| pKP1264 | ExbD(I24C) | Present study |
| pKP1265 | ExbD(D25C) | Present study |
| pKP1284 | ExbD(V26C) | Present study |
| pKP1285 | ExbD(M27C) | Present study |
| pKP1286 | ExbD(L28C) | Present study |
| pKP1395 | ExbD(V29C) | Present study |
| pKP1396 | ExbD(L30C) | Present study |
| pKP1405 | ExbD(L31C) | Present study |
| pKP1397 | ExbD(I32C) | Present study |
| pKP1406 | ExbD(I33C) | Present study |
| pKP1389 | ExbD(F34C) | Present study |
| pKP1386 | ExbD(M35C) | Present study |
| pKP1399 | ExbD(V36C) | Present study |
| pKP1388 | ExbD(A37C) | Present study |
| pKP1390 | ExbD(A38C) | Present study |
| pKP1387 | ExbD(P39C) | Present study |
| pKP1398 | ExbD(L40C) | Present study |
| pKP1391 | ExbD(A41C) | Present study |
| pKP1392 | ExbD(T42C) | Present study |
| pKP1393 | ExbD(V43C) | Present study |
| pKP1412 | ExbD(D25N, L40C) | Present study |
| pKP1413 | ExbD(D25N, A41C) | Present study |
| pKP1445 | ExbD(D25N, T42C) | Present study |
| pKP1406 | ExbD(D25N, V43C) | Present study |
| pKP1191 | ExbD(D25A) | Present study |
| pKP1276 | ExbD(D25A, F23D) | Present study |

| | | |
|---|---|---|
| pKP1273 | ExbD(D25A, I24D) | Present study |
| pKP1201 | ExbD(D25A, V26D) | Present study |
| pKP1213 | ExbD(D25A, M27D) | Present study |
| pKP1229 | ExbD(D25A, L28D) | Present study |
| pKP1202 | ExbD(D25A, V29D) | Present study |
| pKP1413 | ExbD(D25A, L30D) | Present study |
| pKP1272 | ExbD(D25A, L31D) | Present study |
| pKP1277 | ExbD(D25A, I32D) | Present study |
| pKP1287 | ExbD(D25A, I33D) | Present study |
| pKP1288 | ExbD(D25A, F34D) | Present study |
| pKP1322 | ExbD(D25A, M35D) | Present study |
| pKP1351 | ExbD(D25A, V36D) | Present study |
| pKP1359 | ExbD(D25A, A37D) | Present study |
| pKP1349 | ExbD(D25A, A38D) | Present study |
| pKP1360 | ExbD(D25A, P39D) | Present study |
| pKP1214 | ExbD(D25A ,L40D) | Present study |
| pKP1215 | ExbD(D25A, A41D) | Present study |
| pKP1199 | ExbD(D25A, T42D) | Present study |
| pKP1197 | ExbD(D25A, V43D) | Present study |
| pKP2234 | ExbD(T21am) | Present study |
| pKP2235 | ExbD(F23am) | Present study |
| pKP2064 | ExbD(I24am) | Present study |
| pKP2236 | ExbD(D25am) | Present study |
| pKP2229 | ExbD(M27am) | Present study |
| pKP2224 | ExbD(V29am) | Present study |
| pKP2237 | ExbD(I32am) | Present study |
| pKP2065 | ExbD(F34am) | Present study |
| pKP2225 | ExbD(M35am) | Present study |
| pKP2226 | ExbD(A37am) | Present study |

# FIGURES

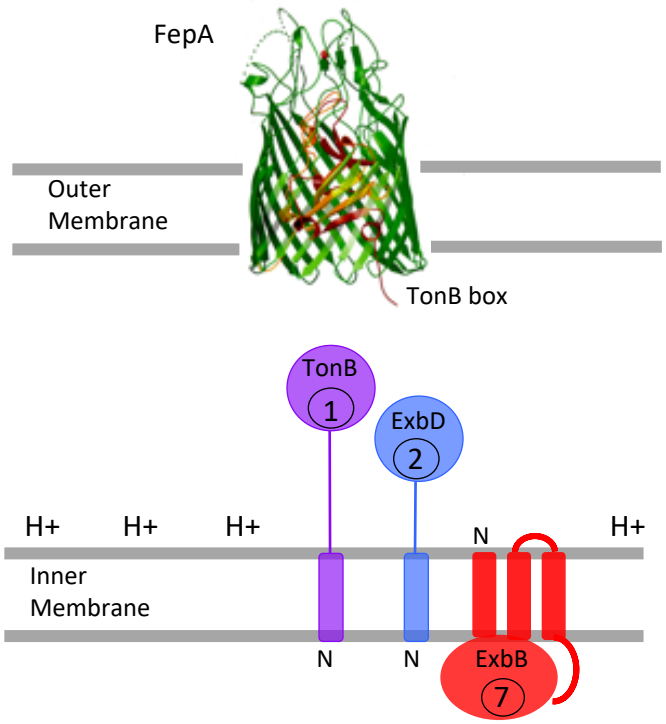


**Figure 1. The TonB system of *Escherichia coli* K12.** The TonB-dependent transporter, FepA, is shown in the outer membrane. At its extreme amino terminus, the TonB box, a site of interaction with TonB, is shown protruding into the periplasm. The topologies of the cytoplasmic membrane proteins TonB, ExbB and ExbD are shown in the cytoplasmic membrane. Cellular ratios of the three proteins are indicated in circles in each protein. The protonmotive force gradient of the cytoplasmic membrane (H+) is shown. The crystal structure of FepA was solved by Buchanan et al. (120).

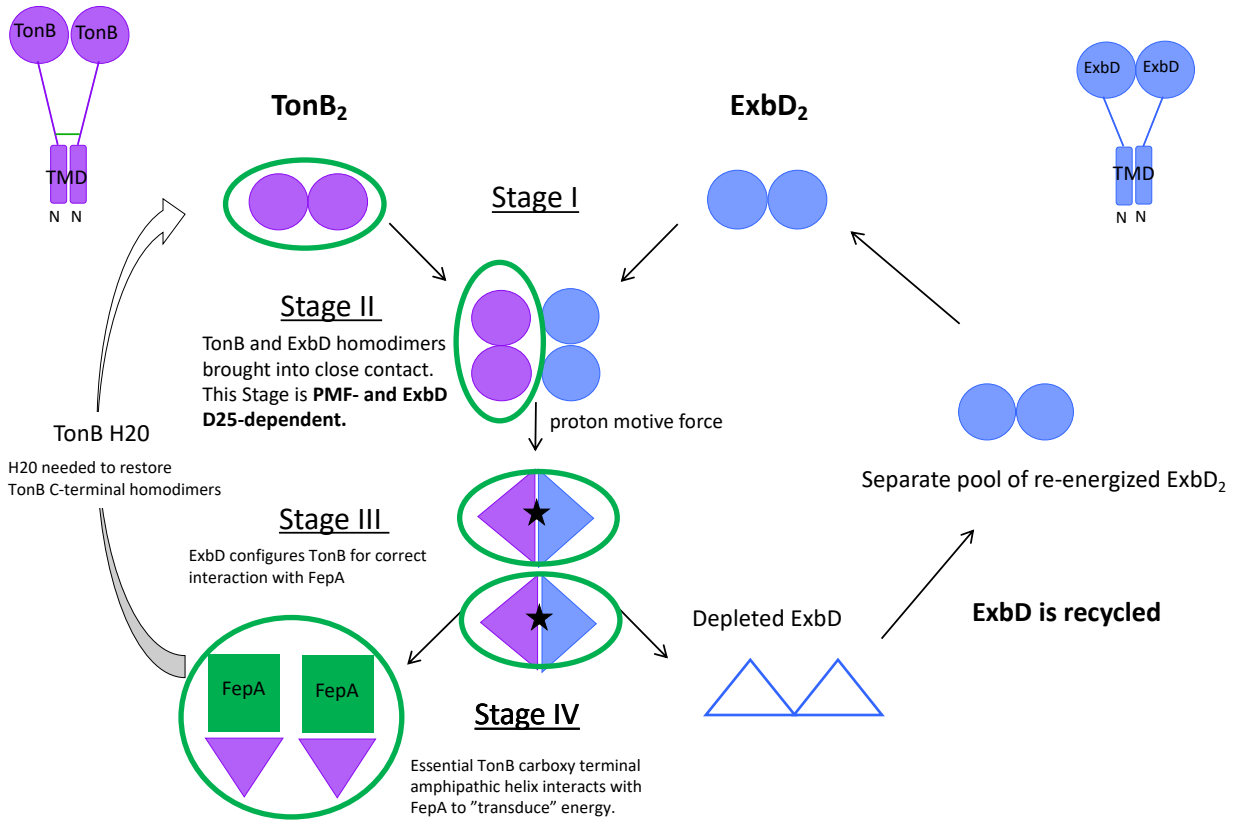


**Figure 2. Model for the TonB energy transduction cycle and the role of ExbD based on *in vivo* data [adapted from (12)].** Full length TonB (purple, upper left corner) and ExbD (blue, upper right corner) each have a single transmembrane domain signal anchor in the cytoplasmic membrane with the bulk of the residues occupying the periplasmic space. The TonB transmembrane domain remains homodimerized throughout the cycle (12). The ExbD transmembrane domain also homodimerizes (as shown in this work), but it is not known if this persists throughout the cycle. Interactions between the periplasmic carboxy-terminal domains of TonB$_2$ and ExbD$_2$ homodimers are shown. Purple circles/triangles are TonB carboxy termini. Blue circles/triangles are ExbD carboxy termini. ExbB tetramers (ExbB$_4$), shown to exist *in vivo*, independently stabilize both TonB and ExbD (23, 80). For simplicity, ExbB$_4$ is not shown in this model. The TonB-

dependent transporter, FepA, is represented by the green square. In Stage I, TonB periplasmic domains form obligatory homodimers through residues in and near its single carboxy terminal amphipathic helix (residues 199-216), mediated by H20 in the TonB TMD, which plays a structural role (12, 26, 41, 72). ExbD periplasmic domains also homodimerize (36). In Stage I there is no evidence that TonB and ExbD homodimers interact, yet both are proteolytically stabilized by ExbB, suggesting that they might exist in separate ExbB tetramers. Such a distribution also helps to account for cellular ratios of 14 ExbB: 4ExbD: 2TonB. In Stage II TonB and ExbD periplasmic domain homodimers are brought into close contact by movement of the ExbB tetramers such that ExbD protects TonB in spheroplasts from degradation by exogenously added protease (36, 42). In Stage III, the previously homodimeric TonBs and ExbD periplasmic domains convert into a dimer of TonB-ExbD heterodimers in spheroplasts that become sensitive to degradation by exogenously added protease (36). Energized ExbD correctly configures TonB for productive interaction with FepA. Stage IV is binding of a monomeric periplasmic domain of TonB to FepA, such that the siderophore enterochelin is actively transported across the outer membrane (18). After a transport event, H20, a key structural residue in the transmembrane domain, is somehow required for re-establishment of TonB periplasmic domain homodimers in Stage I (12, 26, 41). The green circles represent that all stages of the TonB energy transduction cycle involve the participation of the essential carboxy terminal amphipathic helix (residues 199-216) in TonB (18). In this model, the cellular ratios of 14 ExbB: 4ExbD: 2TonB leads to an excess of 2 ExbDs that are not associated with TonB (11). Because TonB functions as an obligate homodimer through its transmembrane domain (12), we speculate that $ExbD_2$ is "de-energized" after Stage IV (empty blue triangles) and is separately recycled. In this model, $ExbD_2$ moves in and out

of interactions with $TonB_2$ escorted by $ExbB_4$ tetramers. A separate pool of recycled $ExbB_4$-$ExbD_2$ is hypothesized to exist to replenish Stage I $ExbB_4$-$ExbD_2$ homodimers. See (12) for a full explanation of the experimental basis for the model.

**Figure 3. The most meaningful sequence comparisons among ExbD paralogues are based on the conserved Asp residue in the transmembrane domains.**

## A. Alignment based on TOPCONS

```
ExbD    21t p f i d v m l v l l i i f m v a a p l a41
TolR    16i n i v p l l d v l l v l l l i f m a t a36
MotB    25s w k i a y a d f m t a m m a f F l v M w45
PomB    23a d l m s l l m c f f v l l l s F s e M d43
```

## B. Alignment based on conserved Asp residue 25 in ExbD

```
ExbD    21t p f i D v m l v l l i i F m v a a p l a t v43
TolR    19v p l l D v l l v l l l i F m a t a p i i t q41
MotB    28i a y A D f M t a m M a F F l v m w l i S i s50
PomB    20g t f A D l M s l l M c F F v l l l s f S e m42
                *                 *
```

A slightly expanded number of possible transmembrane domain residues are considered here to encompass the widest range of options. Alignment based on the conserved Asp residue in B. has been previously proposed (48).

Residues conserved between ExbD and TolR are indicated in bold underline in A and B.

Residues conserved between MotB and PomB are in upper case in both A and B.

Residues conserved in all four proteins in B. are indicated by an asterisk *.

Residues which, as Cys substitutions, cross-link strongly with oxidative catalysis ($I_2$ or cu-*o*-phenanthroline) are highlighted in magenta (46, 47). Cys substitutions in PomB have not been systematically analyzed for cross-links with $I_2$ catalysis (121).

Residues not evaluated as Cys substitutions, but that would be interesting to examine in the context of the results from this study, are in gray (46, 47, 121).

**A.**

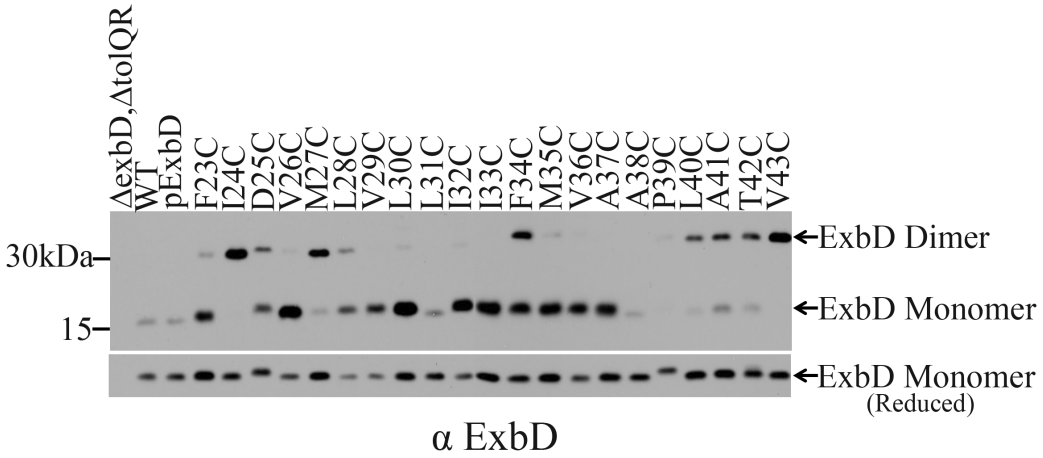


B.

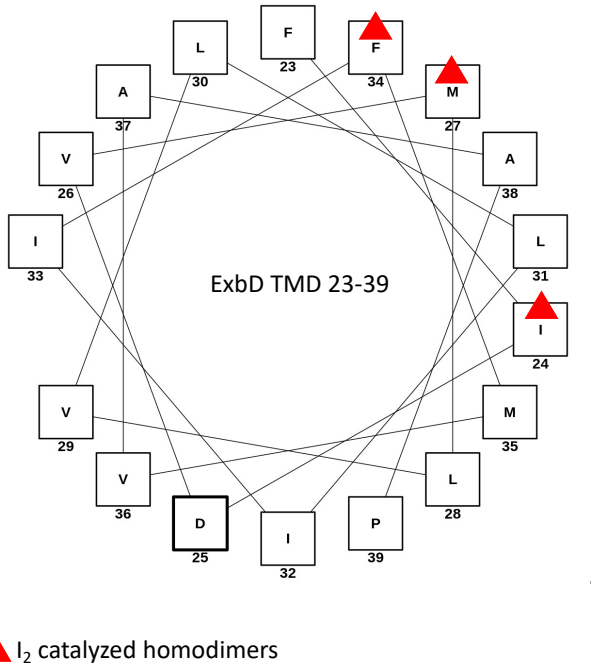


**Figure 4. Oxidized Cys substitutions in the ExbD transmembrane domain define a helical homodimerization face. A.** ExbD Cys substitutions in RA1045 (Δ*exbD*, Δ*tolQR*) were subjected to $I_2$ catalysis as described in Materials and Methods. Divided samples were processed for immunoblotting with anti-ExbD antiserum on a non-reducing SDS

13% polyacrylamide gels. Strains and ExbD variants are indicated at the top of the immunoblot. The position of ExbD monomers and homodimers are indicated on the right with mass markers on the left. WT = W3110; pExbD = pKP999. The corresponding levels of ExbD variants resolved on a reducing SDS 13% polyacrylamide gel are indicated in the lower immunoblot. Equal numbers of cells were loaded in each lane. Two different immunoblots are shown with the partition occurring between ExbD I32C and I33C. **B.** Helical wheel diagram of residues 23-39 of the ExbD transmembrane domain. The most abundant complexes, formed by ExbD I24C, M27C and F34C, are labeled with red triangles and form a face on the helix. Residues 40-43 are not included in the helical wheel analysis since they represent a likely disordered region (see Fig. 5 results).

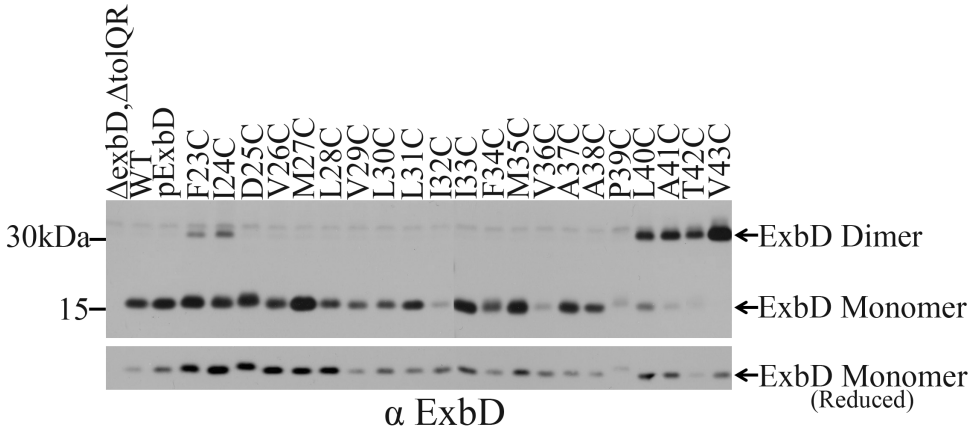


**Figure 5. Spontaneous homodimer formation through ExbD L40C, A41C, T42C, and V43C suggests they are separate from the helical transmembrane domain.** Divided samples of ExbD Cys substitutions in RA1045 (Δ*exbD*, Δ*tolQR*) prepared in the absence of $I_2$ were processed for immunoblotting with anti-ExbD antiserum on non-reducing SDS 13% polyacrylamide gels as described in Materials and Methods (upper). Strains and ExbD variants are indicated at the top of the immunoblot. The position of ExbD monomers and homodimers are indicated on the right with mass markers on the left. WT = W3110; pExbD = pKP999. Two different immunoblots are shown with the partition occurring between ExbD I32C and I33C. The corresponding levels of ExbD variants resolved on a reducing SDS 13% polyacrylamide gel are indicated in the lower immunoblot. Equal numbers of cells were loaded in each lane.

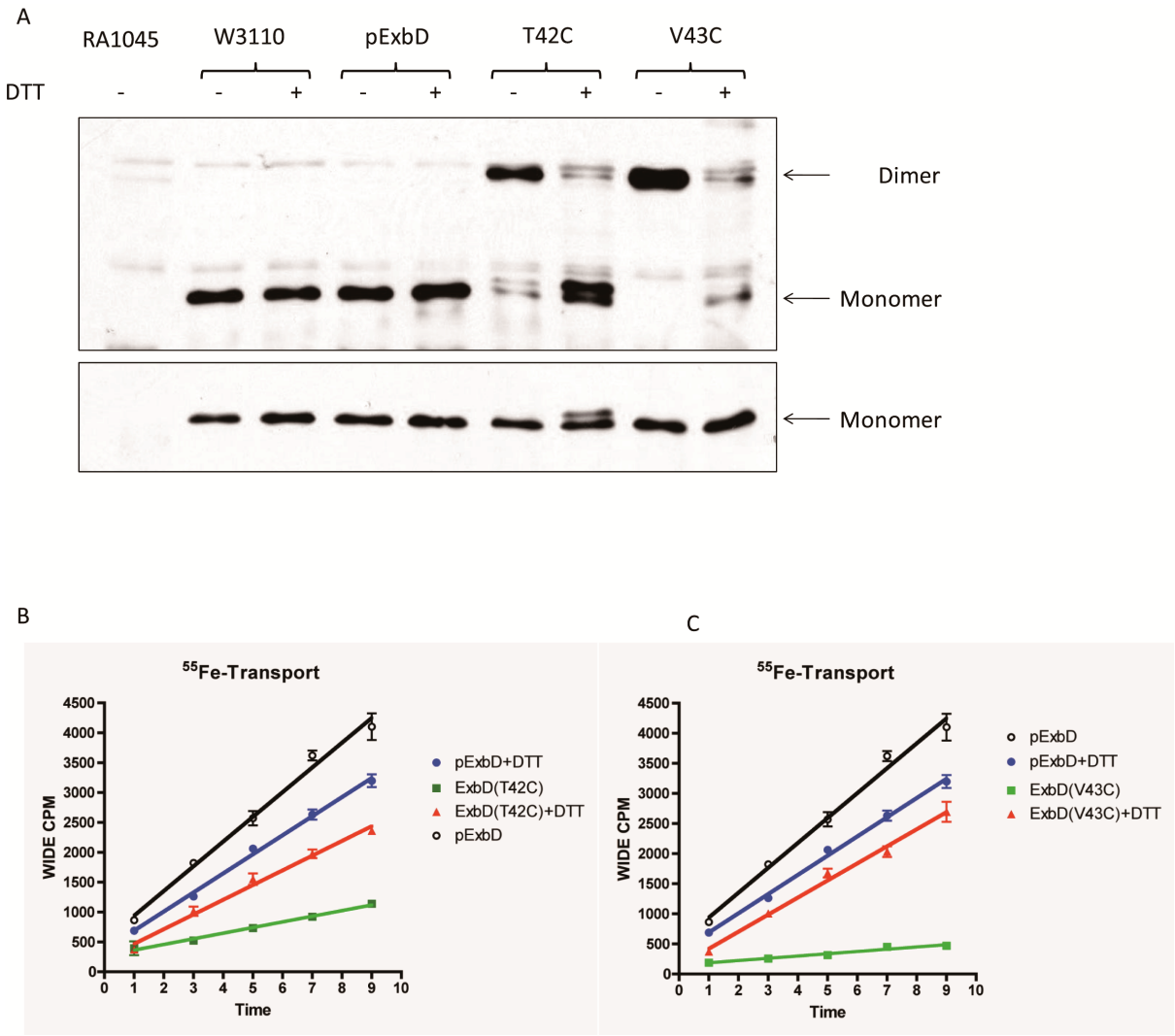


**Figure 6: DTT treatment releases ExbD disulfide-trapped through residues T42C and V43C to support TonB-dependent iron transport. A.** Immunoblot of a non-reducing SDS 13% polyacrylamide gel with anti-ExbD antiserum of the samples evaluated for iron transport. Identity of strains and ExbD variants is indicated at the top. Presence (+) or absence (-) of 2 mM DTT during the logarithmic phase of growth is indicated. The lower panel is an immunoblot of a reducing SDS 13% polyacrylamide gel to determine relative steady state levels of the same samples. Positions of ExbD monomer or dimer are indicated on the right. Equal numbers of cells were loaded in each lane. **B.** Initial rates of iron transport for RA1045 (Δ*exbD*, Δ*tolQR*) cultures with ExbD plasmids, both with and

without DTT. Left panel evaluates plasmids expressing ExbD T42C; right panel evaluates plasmids expressing ExbD V43C. See Table 3 for calculation and comparison of initial rates.

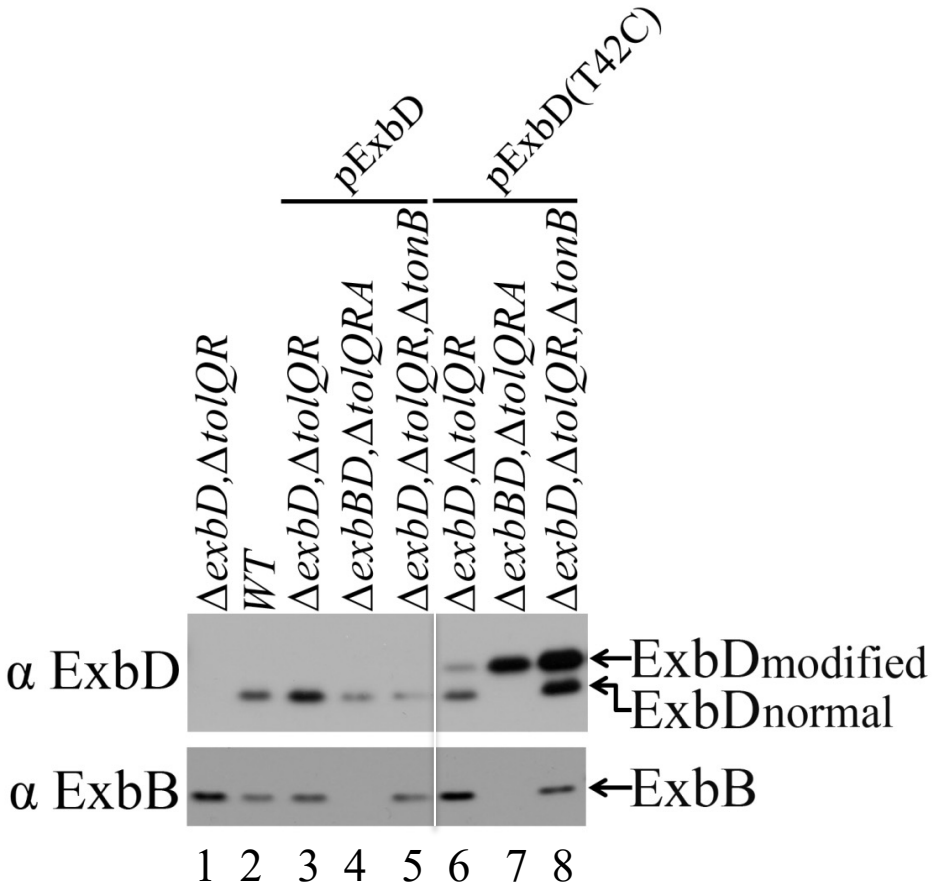


**Figure 7. Apparent *in vivo* modification of ExbDT42C occurs most prominently in the absence of ExbB**. Wild-type plasmid-encoded ExbD (pKP999) or ExbDT42C (pKP1392) were grown as described in Materials and Methods and immunoblotted under reducing conditions with anti-ExbD antibodies (upper panel) or anti-ExbB antibodies (lower panel). The positions of normal and modified ExbD and of ExbB are indicated on the right. Strain genotypes are listed at the top of the immunoblot; WT = W3110. RA1045 is (Δ*exbD*, Δ*tolQR*); RA1017 is (Δ*exbBD*, Δ*tolQRA*); KP1509 is (Δ*exbD*, Δ*tolQR, ΔtonB*). Lane 1, RA1045; lane 2, W3110; lane 3, RA1045/pKP999; lane 4, RA1017/pKP999; lane 5, KP1509/pKP999; lane 6, RA1045/pKP1392; lane 7, RA1017/pKP1392; lane 8,

KP1509/pKP1392. Equal numbers of cells were loaded in each lane. The immunoblots shown for each antibody are from the same exposure with non-relevant lanes removed (indicated by the white line). Amounts of propionate inducer added were: lane 1, none; lane 2, none, lane 3, 0.25 mM; lane 4, 3.0 mM, lane 5, none; lane 6, 0.018 mM; lane 7, 0.02 mM; lane 8, none.

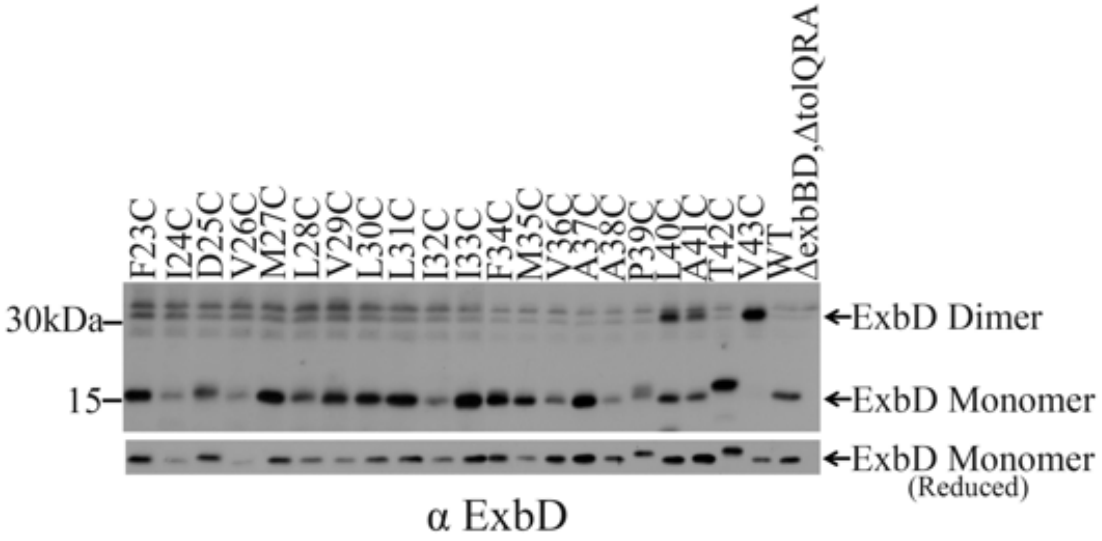


**Figure 8. ExbB is required for homodimerization of full-length ExbD through its transmembrane domain.** ExbD Cys substitutions in RA1017 (Δ*exbBD*, Δ*tolQRA*) were subjected to $I_2$ catalysis as described in Materials and Methods. Divided samples were processed for immunoblotting with anti-ExbD antiserum on non-reducing SDS 13% polyacrylamide gels as described in Materials and Methods (upper). Strains and ExbD variants are indicated at the top of the immunoblot. The position of ExbD monomers and homodimers are indicated on the right with mass markers on the left. WT = W3110. Two different immunoblots are shown with the partition occurring between ExbD I33C and F34C. ExbB T42C did not homodimerize, likely because it was chemically modified in the absence of ExbB (see Fig. 7). The corresponding steady state levels of ExbD variants resolved on a reducing SDS 13% polyacrylamide gel are indicated in the lower immunoblot. Equal numbers of cells were loaded in each lane.

A.

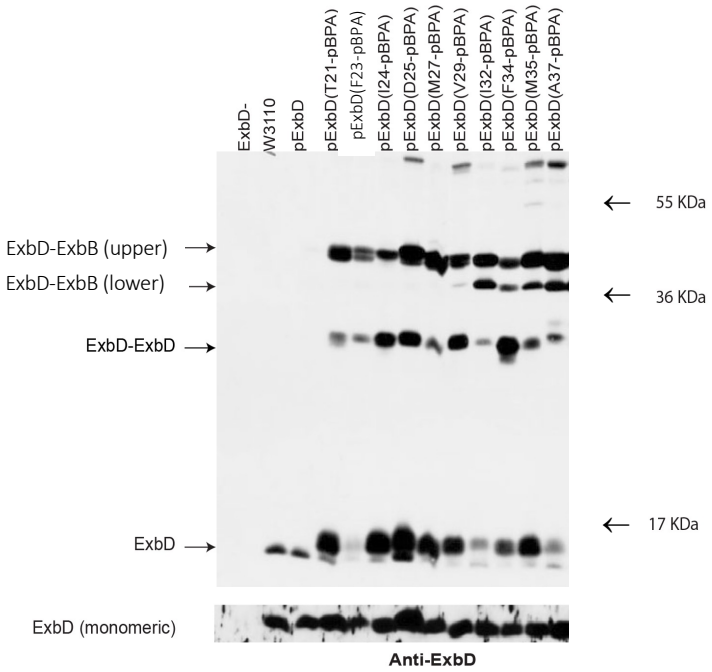


B.

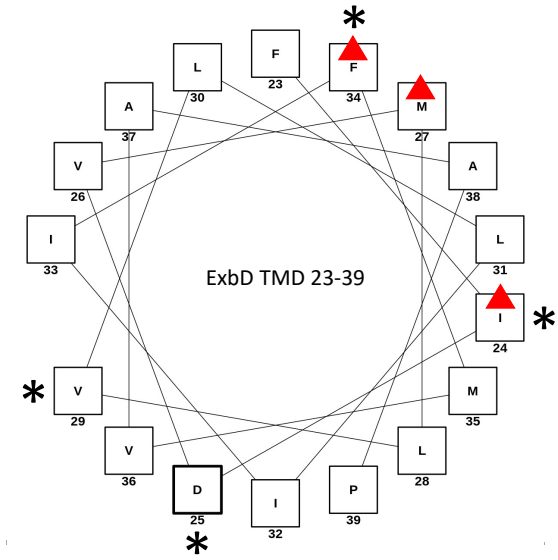


▲ $I_2$ catalyzed homodimers ✱ Photocrosslinked homodimers

**Figure 9. *In vivo* photo-cross-linking suggests that the ExbD helices rotate with respect to one another. A.** ExbD with pBpa incorporated at various codons in the transmembrane domain was subjected to *in vivo* photo-cross-linking as described in Materials and Methods, resolved on an SDS 13% polyacrylamide gel and immunoblotted with anti-ExbD antisera. Strains and substituted ExbD residues are indicated at the top of the upper immunoblot. Strain labeled ExbD- is RA1045 (Δ*exbD*, Δ*tolQR*); pExbD is pKP999; W3110 is wild-type *E. coli*. The position of ExbD monomers, homodimers, and two different previously identified ExbD-ExbB homodimers (59), are indicated on the left with mass markers on the right. Prior to treatment of the samples in A. with ultraviolet light, the level of steady state monomeric ExbD expression and incorporation of pBpA were determined by processing the same volume of sample from A. for immunoblotting with anti-ExbD antiserum on reducing SDS 13% polyacrylamide gels shown in the lower immunoblot. Equal numbers of cells were loaded in each lane. **B.** Helical wheel diagram of residues 23-39 of the ExbD transmembrane domain. The most abundant homodimers formed by *in vivo* photo-cross-linking occurred through ExbD I24pBpa, D25pBpa, V29pBpa, and F34pBpa and are labeled with asterisks. The most abundant disulfide-linked homodimers, formed by ExbD I24C, M27C and F34C, are labeled with red triangles as in Fig. 4. Residues 40-43 are not included in the helical wheel analysis since they represent a likely disordered region (see Fig. 5 results).

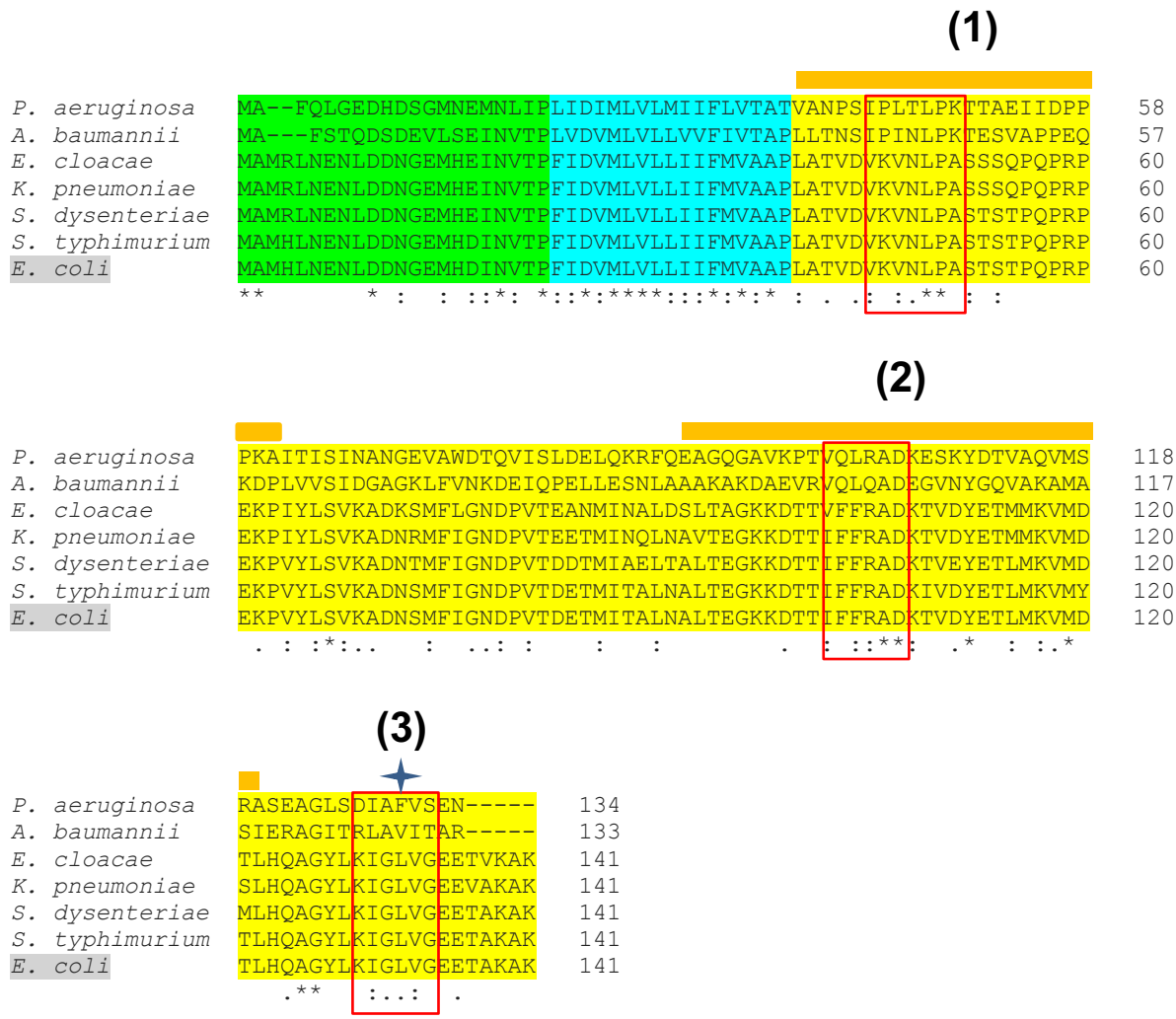


**Figure 10: ExbD sequences chosen as cyclic peptide templates are semi-conserved among several ESKAPE pathogens.** Based on the *E. coli* K12 primary amino acid sequence, the ExbD cytoplasmic domain is highlighted in green, the transmembrane domain is highlighted in blue, and the periplasmic domain is highlighted in yellow. The *E. coli K12 exbD* DNA sequence is identified by the gray highlight in the sequence alignment. The selected ExbD regions from which synthetic cyclic peptides were designed based on *E. coli* K12 sequences are boxed in red. The asterisks (*) below the alignment

identify complete residue conservation; hyphens ( : ) identify conserved residue properties; periods ( . ) identify conserved similar residue properties. The orange bar labeled **(1)** above the alignment identifies the ExbD disordered domain in *E. coli* K12—residues 40-43 from this study plus residues 44-63 from (60). The orange bar labeled **(2)** above the alignment identifies the ExbD residues 92-121 in *E. coli* K12 that are necessary for all known ExbD formaldehyde cross-linked complexes (35). The blue star labeled **(3)** above the alignment identifies the L132 residue shown in this work to be relatively unimportant. The accession numbers are *P. aeruginosa* (AAF04084.1); *A. baumannii* (AOX72224.1); *E. cloacae* (ESS57504.1); *K. pneumoniae* (CDO12443.1); *S. dysenteriae* (ABB63085.1); *S. typhimurium* (TKE83773.1); *E. coli K12* (AAA69172.1). Alignment was generated using Clustal-Omega (1.2.4) multiple sequence alignment (http://www.clustal.org/omega).

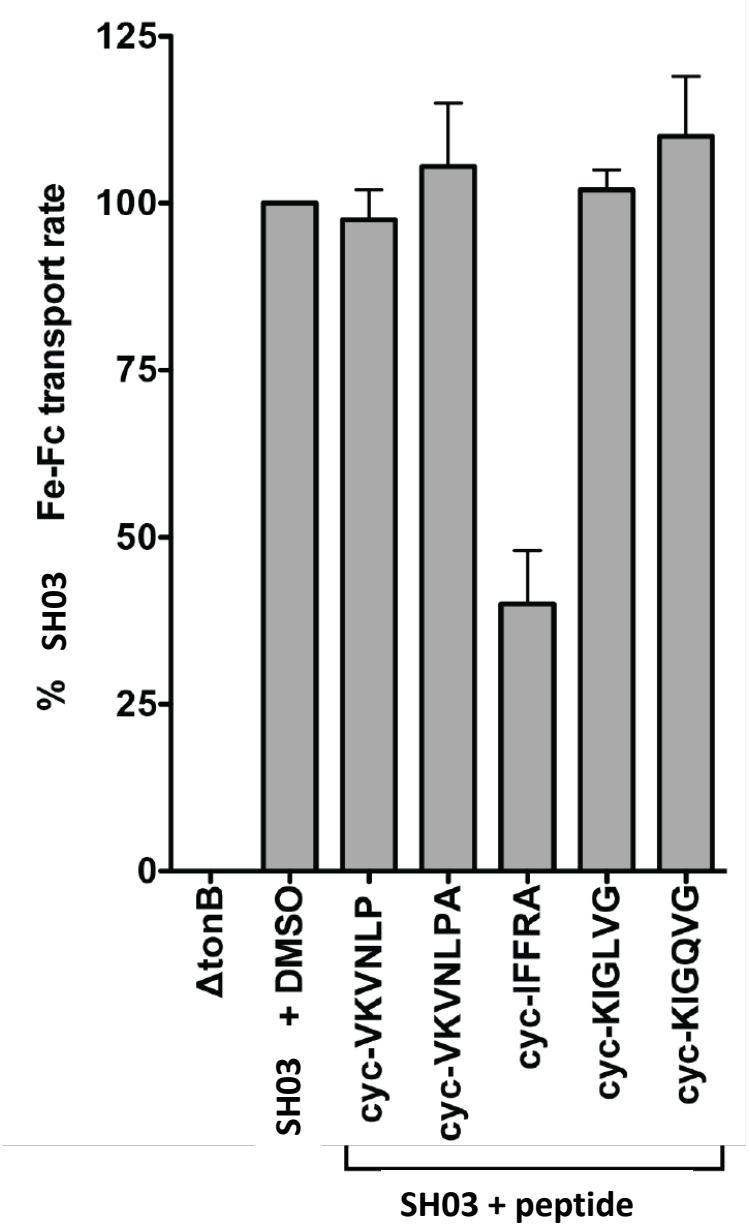


**Figure 11: Cyclic peptide IFFRA inhibits TonB system activity.** The initial rate of $^{55}$Fe-ferrichrome transport by strain SH03 (W3110, *tolC*::Tn*10*) in the presence of dimethyl sulfoxide (DMSO) or synthetic cyclic peptides in DMSO is shown. Cyclic peptide cyc-VKVNLP is based on ExbD residues 45-50; cyc-VKVNLPA is based on ExbD residues 45-51; cyc-IFFRA is based on ExbD residues 102-106, cyc-KIGLVG is based on ExbD residues 129-134, and cyc-KIGQVG is based on ExbD residues 129-134

with an L-to-Q substitution (see Fig. 10). Strains were grown until mid-exponential phase at which point an $A_{550}$ of 1.4 cells were harvested and suspended in assay medium as previously described (115). DMSO or synthetic peptides (500 µM) suspended in DMSO were added, and samples were incubated at 30˚C while shaking for five minutes prior to measuring the initial $^{55}$Fe-ferrichrome transport rate. The $^{55}$Fe-ferrichrome transport rate was recorded as the percent of the SH03 transport rate. Δ*tonB* refers to W3110 with the *tonB* gene deleted [KP1477; (112)]. The error bars indicate mean ± SEM for two biological replicates, each containing three technical replicates.

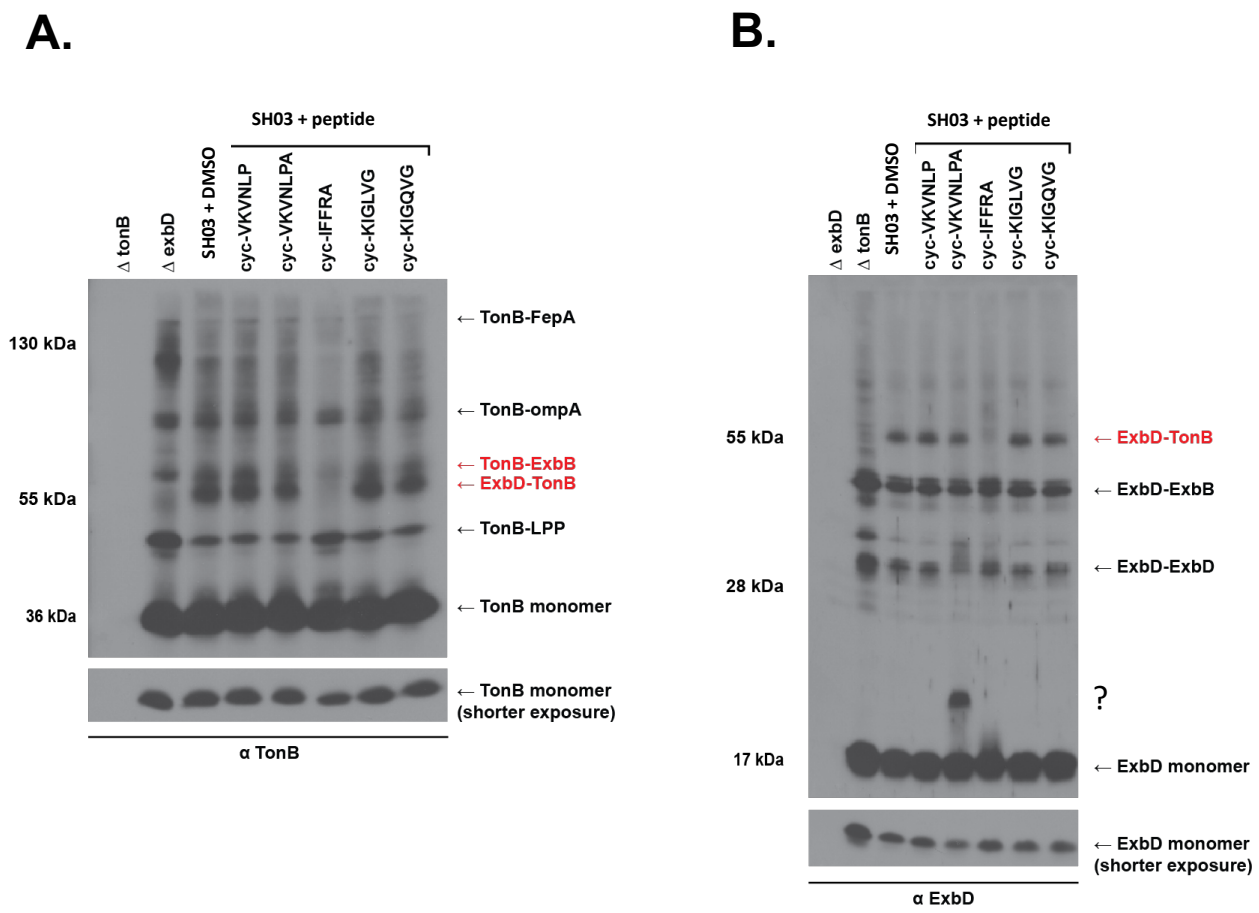


**Figure 12: IFFRA inhibits TonB-ExbD and TonB-ExbB complex formation.** Formaldehyde cross-linking of SH03 (W3110, *tolC*::Tn*10*) in the presence of dimethyl sulfoxide (DMSO) or synthetic cyclic peptides in DMSO is shown. Cyclic peptide cyc-VKVNLP is based on ExbD residues 45-50; cyc-VKVNLPA is based on ExbD residues 45-51; cyc-IFFRA is based on ExbD residues 102-106, cyc-KIGLVG is based on ExbD residues 129-134, and cyc-KIGQVG is based on ExbD residues 129-134 with an L-to-Q substitution (see Fig. 10). Strains were grown to mid-exponential phase, at which point cells were harvested and suspended in 100 mM sodium phosphate buffer (pH 6.8). DMSO or the synthetic cyclic peptides (500 μM in DMSO) were added five minutes prior to formaldehyde cross-linking as previously described (122). Proteins from equivalent numbers of cells from the same cultures were analyzed on immunoblots of SDS 13%

polyacrylamide gels with (A) anti-TonB monoclonal antibodies and (B) anti-ExbD polyclonal antibodies. Identity of samples are indicated at the top of both immunoblots. Δ*exbD* refers to KP1045; Δ*tonB* refers to KP1477. (**A.**) Positions of the previously characterized TonB formaldehyde cross-linked complexes are indicated on the right: TonB-FepA, TonB-OmpA, TonB-ExbB, PMF-dependent TonB-ExbD, and the TonB-LPP complex (14, 28, 29). The position of TonB monomer is also indicated. Mass markers are indicated on the left. (**B.**) Positions of the previously characterized ExbD formaldehyde cross-linked complexes are indicated on the right: PMF-dependent ExbD-TonB complex, ExbD-ExbB complex, and ExbD-ExbD homodimer (29). The position of ExbD monomer is also indicated. The position of a potential complex between monomeric ExbD and the cyc-VKVNLPA peptide is indicated by "?". Mass markers are indicated on the left. Red text identifies the position of TonB-ExbB and ExbD-TonB complexes that are inhibited in the presence of cyc-IFFRA. Beneath A and B are shorter exposures of the immunoblots showing relative levels of monomers.